

Spectral Attributes: Program `spec_cwt`

COMPUTING SPECTRAL COMPONENTS USING THE CONTINUOUS WAVELET TRANSFORM – PROGRAM `spec_cwt`



Contents

Overview: Alternative spectral decomposition algorithms.....	2
Computation flow chart	2
Output file naming convention	4
Invoking the <code>spec_cwt</code> GUI	7
Theory: Gaussian analysis windows and their spectra	10
Theory: Overview of the continuous wavelet transform (CWT)	11
Theory: The forward and inverse CWT	12
Theory: The forward and inverse CWT (continued)	13
Examples of Morlet wavelets.....	13
Spectral magnitude, phase, and voices	16
Displaying 4D (t,f,x,y) data volumes	17
Spectral balancing and spectral bluing GUI parameters.....	22
Example 1: Spectral balancing of the Great South Basin survey	24
Theory: Spectral balancing and spectral bluing.....	26
Statistical measures of the spectra	26
Theory: Statistical measures of the spectra (peak frequency, peak magnitude, and bandwidth).....	28
The peak spectral frequency and peak spectral magnitude.....	28
The spectral bandwidth	28
The peak spectral magnitude above the mean	28
Theory: Statistical measures of the spectra (effective kurtosis and skewness)	29
Spectral kurtosis and effective kurtosis.....	29
Spectral skewness	29
Theory: Spectral response of common impedance changes.....	30
Spectral response of a discrete jump in impedance.....	30
Seismic response of a thin bed embedded in a constant impedance matrix....	Error! Bookmark not defined.
Seismic response of a thin bed embedded in an increasing impedance matrix	Error! Bookmark not defined.
Spectral response of a linear increase in impedance	31

Spectral Attributes: Program **spec_cwt**

Seismic response of a finite ramp of thickness ΔT	31
Theory: Statistical measures of the spectra (Logarithmic slope and roughness).....	32
Spectral roughness.....	32
Example 2: Statistical Measures of the spectra (Great South Basin survey).....	33
Limiting the zone of application	36
Generating output about and between two horizons.....	40
Generating flattened output.....	40
Bandwidth extension.....	42
Theory: Bandwidth extension based on Wavelet Transform Maximum Magnitude Lines (WTMML)	42
Bandwidth extension GUI parameters	43
Phase residues	46
Theory: The Phase Residue.....	47
Example 3: Mapping incised channels using phase residues	48
Computing coherence from different spectral components	52
References.....	54

Overview: Alternative spectral decomposition algorithms

Spectral decomposition methods can be divided into three classes: those that use quadratic forms, those that use linear forms and those that use atom decomposition. Quadratic forms are based on the Wigner-Ville distribution, which can be easily designed but lose the phase components of the data and therefore cannot be used in reconstruction. Linear forms are based on the short time Fourier transform (STFT) and include the S transform and the continuous wavelet transform (or CWT) as in program **spec_cwt**. Program **spectral_probe** is a simple crosscorrelation algorithm that cannot be used to reconstruct the data. Program **spec_max_entropy** is a nonlinear implementation of the short time Fourier transform. Atomic decomposition reconstructs the signal by using small “atom-sized” signals (in our case wavelets), such as matching pursuit (program **spec_cmp**) and the Hilbert-Huang transform.

Computation flow chart

While there is in general only one input file to program **spec_cwt**, many output files can easily fill your disk drives. Detailed spectral analysis will typically be done about a reservoir or other zone of interest, such that the input data volume may be windowed. If the data have not previously been spectrally whitened, it may be beneficial to reconstruct the spectrally balanced amplitude. In either case, it is best to ask for spectrally balanced spectral components and statistical

Spectral Attributes: Program `spec_cwt`

measures; balancing will suppress the effect of the dominant frequency of the source wavelet, leaving the tuning effects of the geology in place.

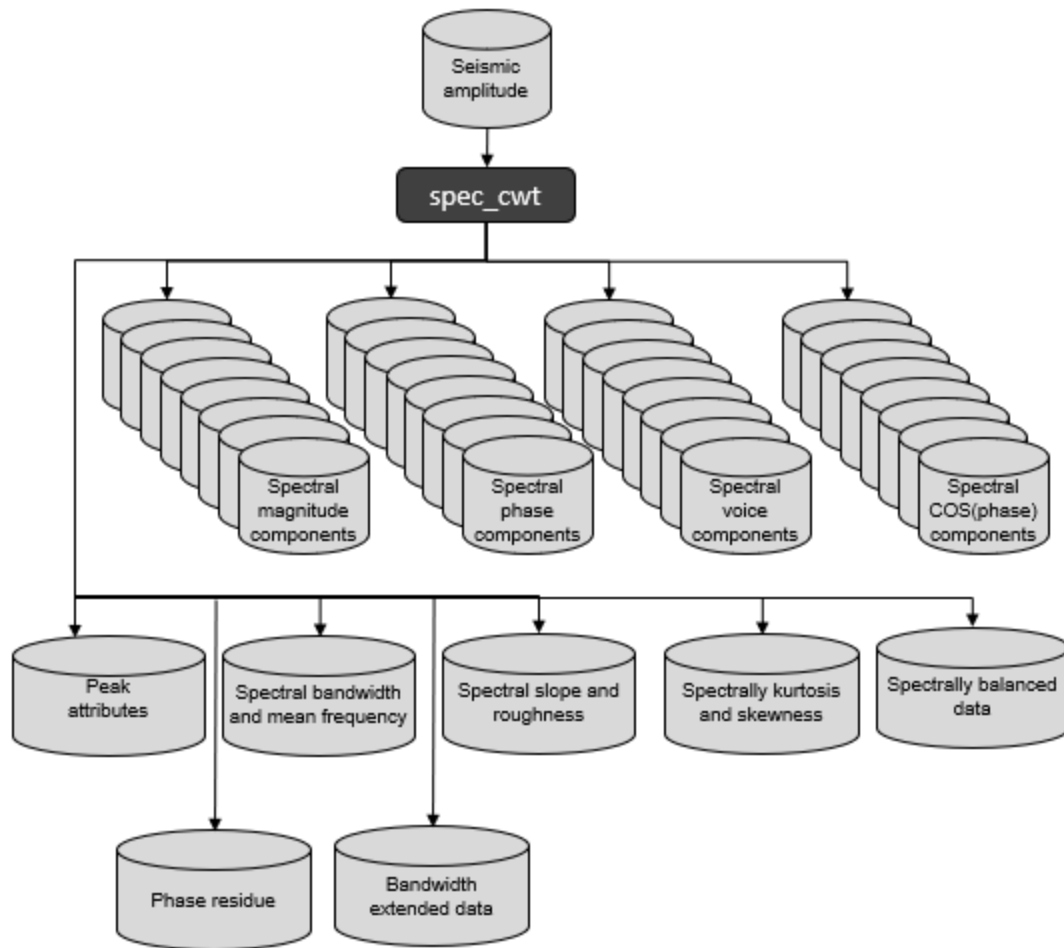


Figure 1.

The `spec_cwt` workflow showing input and output volumes.

Spectral Attributes: Program **spec_cwt**

Output file naming convention

Program **spec_cwt** will always generate the following output files:

Output file description	File name syntax
Complex wavelets	<code>complex_cwt_wavelet_unique_project_name_suffix.H</code>
Program log information	<code>spec_cwt_unique_project_name_suffix.log</code>
Program error/completion information	<code>spec_cwt_unique_project_name_suffix.err</code>

where the values in red are defined by the program GUI. The errors we anticipated will be written to the *.err file and be displayed in a pop-up window upon program termination. These errors, much of the input information, a description of intermediate variables, and any software trace-back errors will be contained in the *.log file.

If the want peak attributes check box is selected, **spec_cwt** will also generate these output files:

Output file description	File name syntax
Peak spectral magnitude	<code>peak_mag_cwt_unique_project_name_suffix.H</code>
Frequency at peak spectral magnitude ("tuning frequency")	<code>peak_freq_cwt_unique_project_name_suffix.H</code>
Phase at peak spectral magnitude	<code>peak_phase_cwt_unique_project_name_suffix.H</code>
Peak magnitude measured above the average(range-trimmed mean) spectral magnitude	<code>peak_mag_above_average_cwt_unique_project_name_suffix.H</code>

If the *Want statistical attributes* box is checked, you will obtain the following files:

Output file description	File name syntax
Range-trimmed mean (average) spectral magnitude	<code>rtm_mag_unique_project_name_suffix.H</code>
Spectral magnitude-weighted mean frequency	<code>mean_freq_cwt_unique_project_name_suffix.H</code>
Slope of the magnitude spectrum	<code>slope_cwt_unique_project_name_suffix.H</code>
Roughness (deviation from a linear trend) of the magnitude spectrum	<code>roughness_cwt_unique_project_name_suffix.H</code>
Spectral bandwidth	<code>Spectral_bandwidth_cwt_unique_project_name_suffix.H</code>

Spectral Attributes: Program **spec_cwt**

Spectral effective kurtosis	<code>effective_kurtosis_cwt_unique_project_name_suffix.H</code>
Spectral skewness	<code>skewness_cwt_unique_project_name_suffix.H</code>

If the data are to be spectrally balanced, you will obtain the following files:

Output file description	File name syntax
Reconstructed seismic data (with or without spectral balancing)	<code>d_recon_cwt_unique_project_name_suffix.H</code>
Average survey time-frequency spectrum before and after balancing	<code>average_magnitude_spectrum_cwt_unique_project_name_suffix.H</code>
Average survey time-frequency scale applied in balancing	<code>average_scale_spectrum_cwt_unique_project_name_suffix.H</code>

Optionally, we can also output a spectral voice, magnitude, and/or phase volume for each decomposition frequency. These files take no longer to generate but may increase i/o time and fill up disk space. In general, consider windowing the range of the output volumes. More modern interpretation workstations allow the visualization of 4D volumes, which will be:

Output file description	File name syntax
Spectral voice components	<code>spec_voice_4d_cwt_unique_project_name_suffix.H</code>
Spectral magnitude components	<code>spec_mag_4d_cwt_unique_project_name_suffix.H</code>
Spectral phase components	<code>spec_phase_4d_cwt_unique_project_name_suffix.H</code>

Other software systems, or a specific interpretation workflow will more easily analyze the spectral components as individual volumes, where the frequency value is appended to the file name:

Output file description	File name syntax
Spectral voice components	<code>spec_voice_3d_cwt_unique_project_name_suffix_frequency.H</code>
Spectral magnitude components	<code>spec_mag_3d_cwt_unique_project_name_suffix_frequency.H</code>
Spectral phase components	<code>spec_phase_3d_cwt_unique_project_name_suffix_frequency.H</code>

If you invoke the bandwidth extension option, you can likewise examine spectral voice and ridge components as single 4D volumes:

Spectral Attributes: Program **spec_cwt**

Output file description	File name syntax
Bandwidth extension spectral voice components	<i>spec_voice_bwe_4d_cwt_unique_project_name_suffix.H</i>
Bandwidth extension spectral ridge components	<i>spec_ridge_bwe_4d_cwt_unique_project_name_suffix.H</i>

or as multiple3D volumes:

Output file description	File name syntax
Bandwidth extension spectral voice components	<i>spec_voice_bwe_3d_cwt_unique_project_name_suffix_frequency.H</i>
Bandwidth extension spectral ridge components	<i>spec_ridge_bwe_3d_cwt_unique_project_name_suffix_frequency.H</i>

The primary output of bandwidth extension is the bandwidth-extended seismic amplitude volumes, along with other files that may be useful in better understanding the process used:

Output file description	File name syntax
Bandwidth extended seismic data volume	<i>d_bandwidth_extension_cwt_unique_project_name_suffix.H</i>
Residual (unmodelled) seismic data using wavelet transform maximum modulus line bandwidth extension	<i>d_residual_cwt_unique_project_name_suffix.H</i>
Bandwidth extended spectral voices	<i>spec_voice_bwe_unique_project_name_suffix.H</i>
Complex wavelets used in bandwidth extension forward transform	<i>complex_bwe_forward_wavelet_cwt_unique_project_name_suffix.H</i>
Complex wavelets used in bandwidth extension inverse transform	<i>complex_bwe_inverse_wavelet_cwt_unique_project_name_suffix.H</i>
Complex wavelet magnitude spectra used in bandwidth extension forward transform	<i>complex_bwe_forward_spectrum_cwt_unique_project_name_suffix.H</i>
Complex wavelet magnitude spectra used in bandwidth extension inverse transform	<i>complex_bwe_inverse_spectrum_cwt_unique_project_name_suffix.H</i>

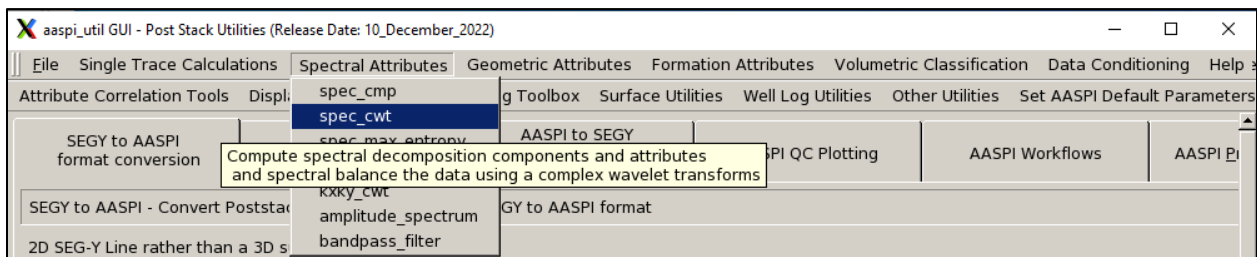
Spectral Attributes: Program **spec_cwt**

Finally, if you choose to generate the phase residues, there will be two additional files:

Output file description	File name syntax
Volume containing the magnitude of any phase residues	phase_residue_mag_cwt_unique_project_name_suffix.H
Volume containing the frequency of any phase residues	phase_residue_freq_cwt_unique_project_name_suffix.H

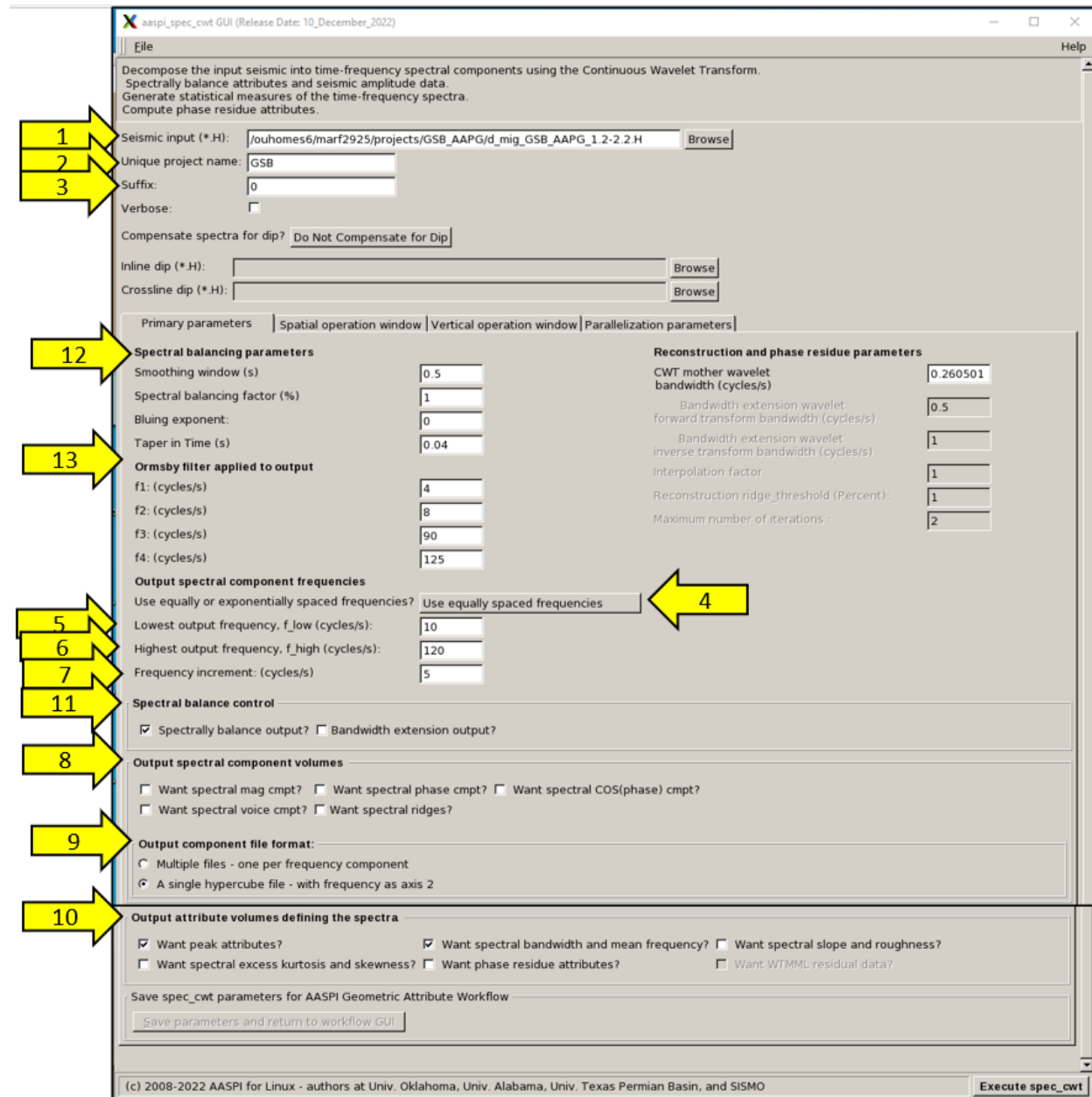
Invoking the **spec_cwt** GUI

To begin, click the *Spectral Attributes* tab in the **aaspi_util** GUI and select program **spec_cwt**:



Program **spec_cwt** performs spectral decomposition by using a continuous wavelet transform method. The following window appears:

Spectral Attributes: Program `spec_cwt`



First, enter the (1) name of the *Seismic Input (*.H)* file you wish to decompose, as well as a (2) *Unique Project Name* and (3) *Suffix* as you have done for other AASPI programs. If you (4) select *Use equally spaced frequencies*, the decomposition will generate data between (5) f_{low} and (6) f_{high} at (7) increments of Δf . Alternatively, click (4) and choose a fixed number of frequencies per octave. One can generate (8) multiple spectral components as either (9) multiple 3D volumes (one per frequency) or as a single 4D ($t, f, CDP_no, Line_no$) volume. More commonly, one will generate some (10) simple spectral statistical measures of the spectrum where the peak frequency, peak magnitude, peak phase, mean frequency, spectral bandwidth, spectral slope, roughness, excess kurtosis, skewness, and phase residue are described in the theory sections below. In almost all cases, you should (11) spectrally balance the data to statistically remove the

Spectral Attributes: Program **spec_cwt**

wavelet spectrum thereby better representing the spectrum of the underlying stratigraphy. (We will return to spectral balancing and its (12) parameters later in this documentation).

For prestack gathers, there will be a time-frequency distribution for every trace, resulting in 5D output for input gathers of the form $(t, h, CDP_no, Line_no)$ or 6D output for input gathers of the form $(t, \varphi, h, CDP_no, Line_no)$ where h is the offset bin and φ is the azimuth bin. Finally (13) f_1, f_2, f_3 and f_4 define the corner frequencies of an Ormsby filter used in spectral balancing and data reconstruction.

Theory: Gaussian analysis windows and their spectra

Teolis (1984) defines the continuous wavelet transform to be based on scaled and shifted versions of a “mother” Morlet wavelet, ψ_M , centered about time $t=0$, which is simply a complex exponential of frequency f_c , within a Gaussian temporal window using a variable γ_b :

$$\psi_M(t, f_c, \gamma_b) = \sqrt{\frac{1}{\pi\gamma_b}} \exp(i2\pi f_c t) \exp\left(-\frac{t^2}{\gamma_b}\right). \quad (1)$$

Teolis (1998) and others (including implementations in Matlab) state that γ_b defines the bandwidth of the resulting spectrum. However, it is by no means a direct definition of the bandwidth as used by the signal analysis community, in part because its units are in seconds rather than in Hz, and in part because it defines a width in the time domain rather than in the frequency domain. To better define the bandwidth, let’s use the Gaussian,

$$g(t, \sigma_t) = \frac{1}{\sqrt{2\pi}\sigma_t} \exp\left(-\frac{t^2}{2\sigma_t^2}\right) \quad (2)$$

where now we see that

$$\gamma_b = 2\sigma_t^2. \quad (3)$$

The Fourier transform of equation 2 is;

$$G(f, \sigma_f) = \exp\left(-\frac{f^2}{2\sigma_f^2}\right), \quad (4)$$

where

$$\sigma_t \sigma_f = \frac{1}{2\pi}. \quad (5)$$

Traditionally, the bandwidth is defined as the spectral distance between the two half-power points of the spectrum. Squaring equation 4 to obtain the power and setting this value to $\frac{1}{2}$ gives,

$$G^2(f_{B/2}, \sigma_f) = \exp\left(-\frac{f_{B/2}^2}{\sigma_f^2}\right) = \frac{1}{2}, \quad (6)$$

where $f_{B/2}$ is the half bandwidth. Taking the natural logarithm of both sides gives the half bandwidth as ,

$$f_B^2 = \ln(2)\sigma_f^2. \quad (7)$$

The full bandwidth is then

$$f_B = 2\sqrt{\ln(2)}\sigma_f. \quad (8)$$

and

$$\frac{1}{\sigma_t} = 2\pi\sigma_f = \frac{2\pi}{2\sqrt{\ln(2)}} f_B = \frac{\pi}{\sqrt{\ln(2)}} f_B. \quad (9)$$

In this manner, the mother wavelet at frequency f_c in equation 1 becomes

$$\psi_M(t, f_c, f_B) = \sqrt{\frac{\pi}{2\ln(2)}} f_B \exp(i2\pi f_c t) \exp\left(-\frac{t^2 \pi^2}{2\ln(2)} f_B^2\right). \quad (10)$$

Theory: Overview of the continuous wavelet transform (CWT)

Formally introduced by Grossmann and Morlet (1984), a function with zero mean is called a “wavelet” if it has finite energy concentrated in time and satisfies certain well-established conditions. A family of wavelet functions can be obtained from a basis (or “mother”) wavelet $\psi_M(t)$ centered about time $t = 0$, by scaling it by a dilation factor s and shifting it by time u :

$$\mathcal{Y}(t, u, s) = \frac{1}{\sqrt{s}} \mathcal{Y}_M \left(\frac{t - u}{s} \right) \tag{11}$$

Mallat (2009) uses the Fourier transform scaling property to show that if $\Psi(f)$ is the Fourier transform of the wavelet $\psi(t)$, then the Fourier transform of the same wavelet scaled by s , $\psi_M(t/s)$, is given by $|s| \Psi(f)$ where f indicates the temporal frequency measured in cycles/s (Hz). Therefore, if we compress the wavelet by increasing s , its spectrum will dilate, and the peak frequency will shift to a higher value. In contrast, if we dilate a wavelet by decreasing s , its spectrum will compress, and the peak frequency will shift to a lower value. For this reason, by varying the scaling factor s , such a wavelet family can represent broadband spectra. In addition, the spectrum of each wavelet in the family maintains a constant ratio between its peak frequency and the corresponding bandwidth. Once a wavelet family is chosen, then the continuous wavelet transform $D(u, s)$ of a function $d(t)$ at time u and scale s is defined as,

$$D(u, s) = \int_{-\infty}^{+\infty} d(t) \frac{1}{\sqrt{s}} \psi_M^* \left(\frac{t - u}{s} \right) dt = d(t) * \psi(t, u, s) \tag{12}$$

where the first superscript $*$ indicates the complex conjugate and the second multiplicative $*$ indicates convolution.

Thus, the CWT algorithm can be implemented by simply convolving, in the time or frequency domain, the seismic trace with a reversed and scaled wavelet $\psi(t, u, s)$. Because the spectrum of $\psi(t, u, s)$ resembles a band-pass filter, the CWT can also be interpreted as the application of a suite of filter banks to the original data, $d(t)$. In order to reconstruct the data, the values of s should be chosen to span the spectrum of the original seismic data.

In seismic exploration, we often model zero-offset seismic traces by convolving the earth’s reflectivity series with a Ricker wavelet. For that reason, a Ricker wavelet centered about 1 Hz provides a good mother wavelet. Another common wavelet was proposed by Morlet et al. (1982), who used a complex sinusoid with frequency f_c modulated by a Gaussian function with variance σ_t^2 :

$$\psi(t, u, s) = \frac{1}{\sigma_t \sqrt{\pi s}} \exp \left[\frac{i 2 \pi f_c (t - u)}{s} \right] \exp \left[- \left(\frac{t - u}{\sigma_t s} \right)^2 \right]. \tag{13}$$

Defining the scale in terms of the j^{th} frequency, $s = 1/f_j$, and using equation 10 this becomes,

$$\psi(t, u, f_j) = \sqrt{\frac{\pi}{2 \ln(2)}} f_B \exp \left[i 2 \pi f_c f_j (t - u) \right] \exp \left[- \frac{\pi^2}{2 \ln(2)} (f_B f_j (t - u))^2 \right]. \tag{14}$$

In the frequency domain, the Morlet wavelet represented by equation 14 is a band-pass filter centered at $f_c f_j$ Hz with half-bandwidth of $f_B/2 f_j$ Hz. Figure A1 shows the real part of the Morlet wavelets and their spectra for both spectral decomposition and for bandwidth extension. In theory, the spectrum of the Morlet wavelet is not zero for zero frequency and cannot be used in the CWT. In practice, most seismic data are missing the lowest frequencies, so the resulting small amount of aliasing can be tolerated when computing the CWT. It is also important to compute a sufficiently dense CWT spectrum to allow a good inverse CWT reconstruction.

Theory: The forward and inverse CWT

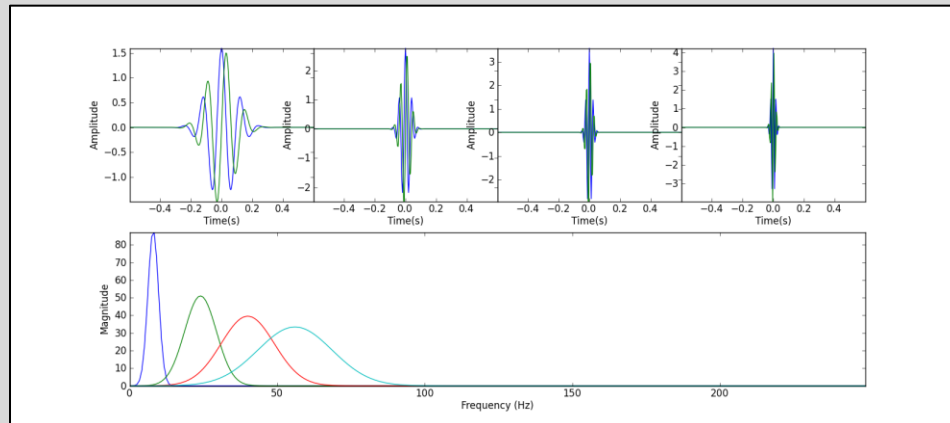


Figure A1. (Top) A suite of four complex Morlet wavelets centered about 10, 20, 40, and 60 Hz with the real part in blue and the imaginary part in green. (Bottom) Their corresponding magnitude spectra at 10 Hz (blue), 20 Hz (green), 40 Hz (red), and 60 Hz (cyan). By construction the bandwidth increases proportionately to the center frequency.

Since the Morlet wavelet is a complex function, the CWT spectral components are also complex. Figure A2 shows the CWT of a seismic trace. The CWT magnitude represents the square root of the energy that correlates with the trace, while the CWT phase represents the phase rotation between the seismic trace and the Morlet wavelet at each instant of time. Goupillaud et al. (1984) showed that the CWT preserves the signal energy and is invertible, such that the signal can be reconstructed from the CWT coefficients as a convolution along the scales plus an integration along time,

$$d(t) = \int_{-\infty}^{+\infty} D(u, s) \frac{1}{\sqrt{s}} \psi_M \left(\frac{t-u}{s} \right) ds = D(u, s) * \psi^*(t, u, s). \tag{15}$$

Perfect reconstruction is achieved for the continuous case, when, theoretically, $d(t)$, u and s are infinitely dense. In practice, we need to sample sufficiently the CWT by the scale, s , to allow a good inverse CWT reconstruction in equation 15 (Goupillaud et al., 1984; Li and Ulrych, 1999). Figure A2d shows the CWT of a seismic trace and the corresponding inverse CWT, or ICWT, reconstruction using equation 15. Figure A2e shows the error in the reconstruction.

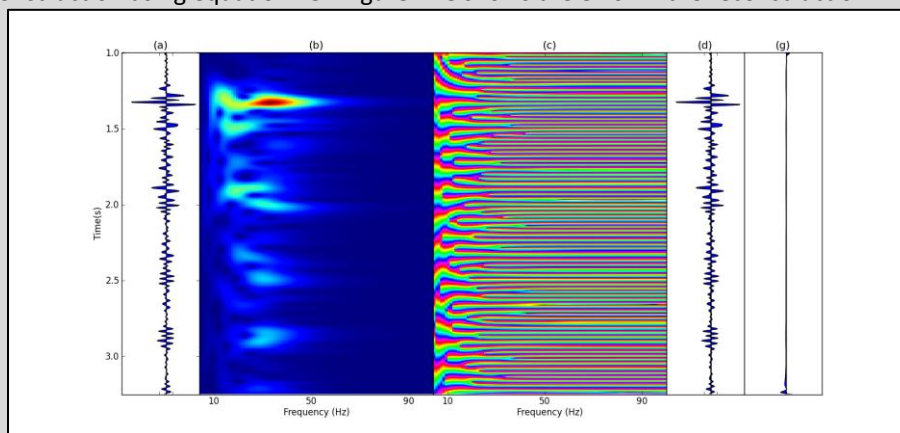


Figure A2. (a) Seismic trace and corresponding CWT (b) magnitude and (c) phase computed using a Morlet mother wavelet with center frequency $f_c=1.0$ Hz and half-bandwidth $f_{B/2}=0.265$ Hz. (c) CWT phase. (d) The inverse CWT (e) the error in reconstruction.

Theory: The forward and inverse CWT (continued)

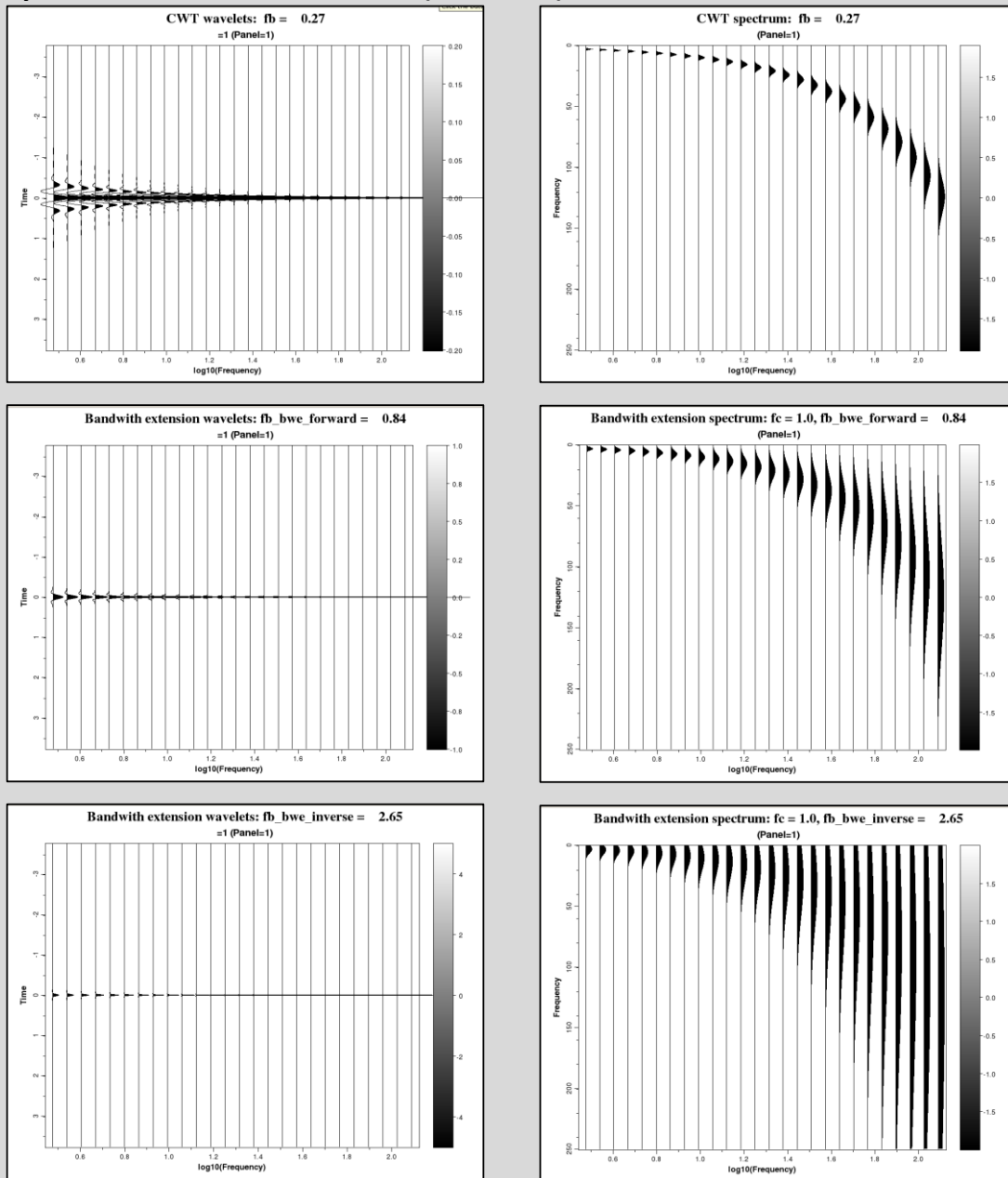


Figure 2. (Left) Real part of the complex wavelets and (Right) their corresponding spectra. (Top row) Narrow-band wavelets used in the forward transform to generate spectral components, statistical attributes, and in the inverse transform to perform spectral balancing. (Middle row) Broadband wavelets used in the forward transform for bandwidth extension. (Bottom row) Very broadband wavelets applied to the spectral modulus maxima ridges in the inverse transform to perform bandwidth extension.

Examples of Morlet wavelets

As described in the gray theory box, the “mother” wavelet is defined by a center frequency, f_c , and a bandwidth, f_B . Other members of the wavelet family are scaled and shifted versions of the

Spectral Attributes: Program `spec_cwt`

mother wavelet. Figures 3-5 show representative wavelets constructed from a moderate band, narrow band, and broad band mother wavelets. The choice of which wavelet to use depends on the application. Liner et al. (2004) used narrow band wavelets in estimate spectral magnitude discontinuities based on a Hölder transform. Singleton et al. (2006) also used narrow band wavelets in their Q estimation work.

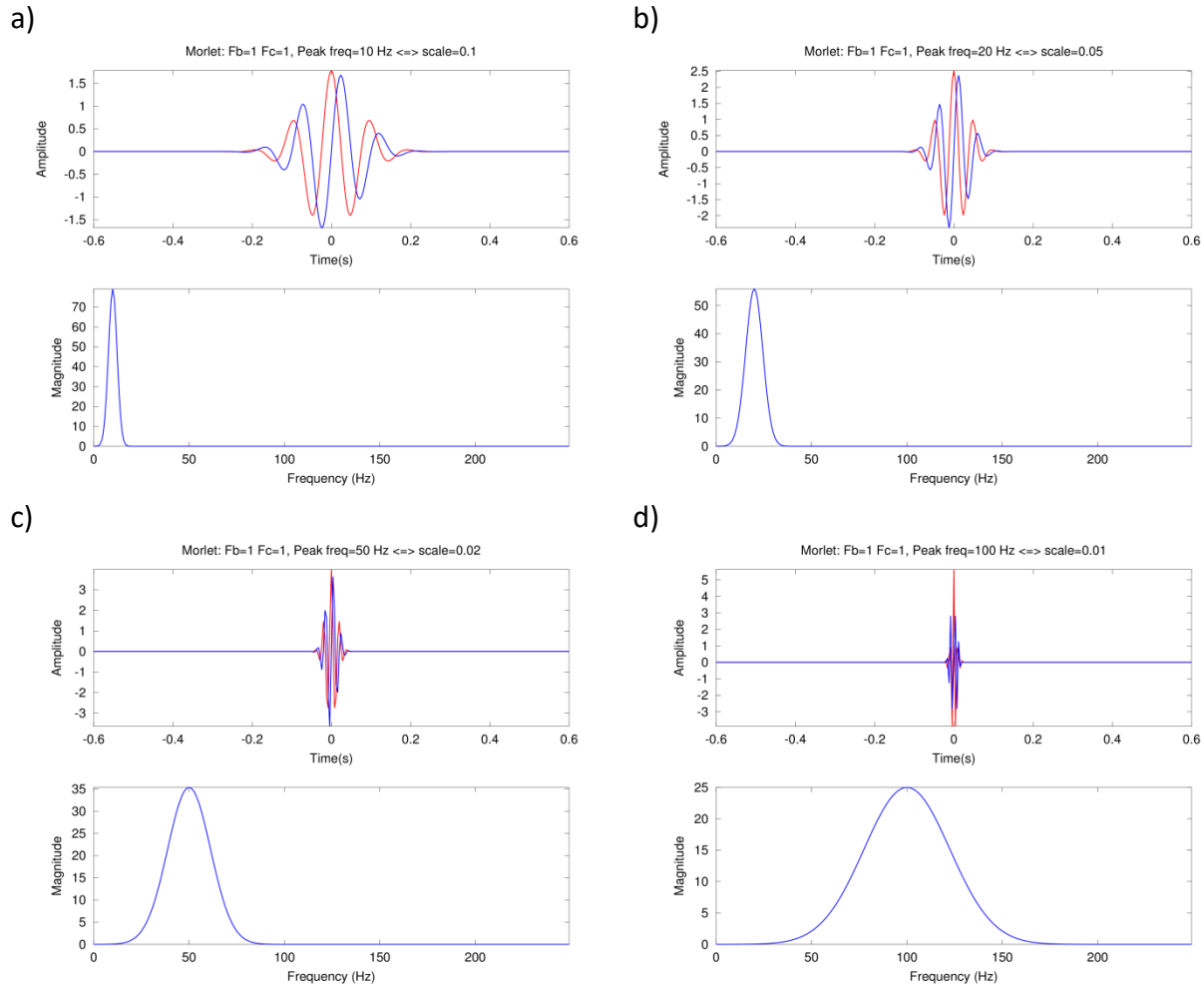


Figure 3. A suite of Morlet wavelets plotted with center frequencies of (a) 10 Hz, (b) 20 Hz, (c) 50 Hz, and (d) 100 Hz. In program `spec_cwt` the default mother wavelet is defined with center frequency $f_c=1.0$ Hz and a half-bandwidth $f_{B/2}=0.265$ Hz (variance $\sigma_t^2=1.00$ s²) giving rise to moderate temporal and frequency resolution.

Spectral Attributes: Program `spec_cwt`

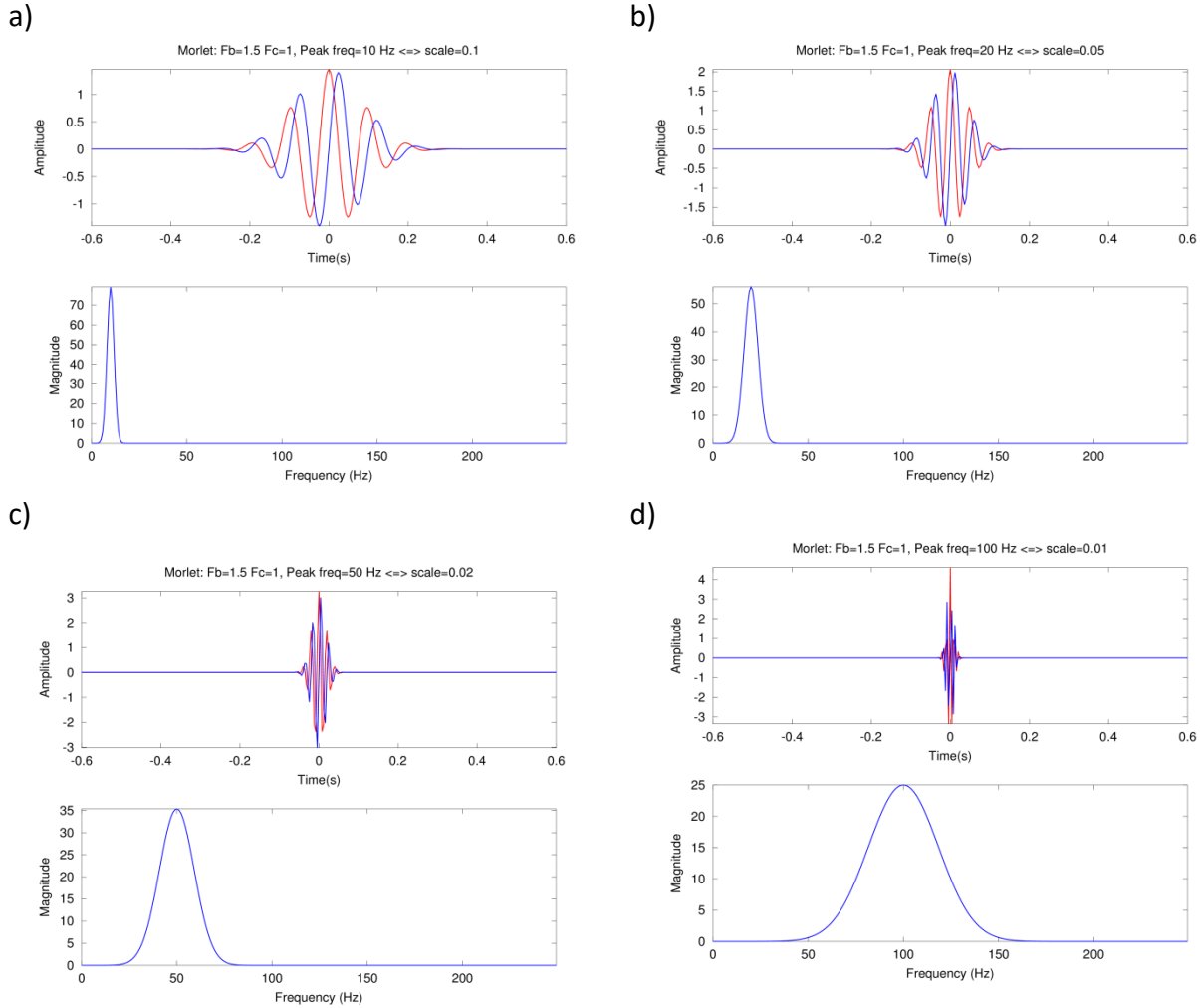


Figure 4. A suite of Morlet wavelets plotted with center frequencies (a) 10 Hz, (b) 20 Hz, (c) 50 Hz, and (d) 100 Hz. The narrow band mother wavelet in this example is defined with center frequency $f_c=1.0$ Hz and half-bandwidth $f_{B/2}=0.187$ Hz (variance $\sigma^2=0.44$ s²), giving rise to a low temporal resolution, but higher frequency resolution than those shown in Figure 3.

Spectral Attributes: Program `spec_cwt`

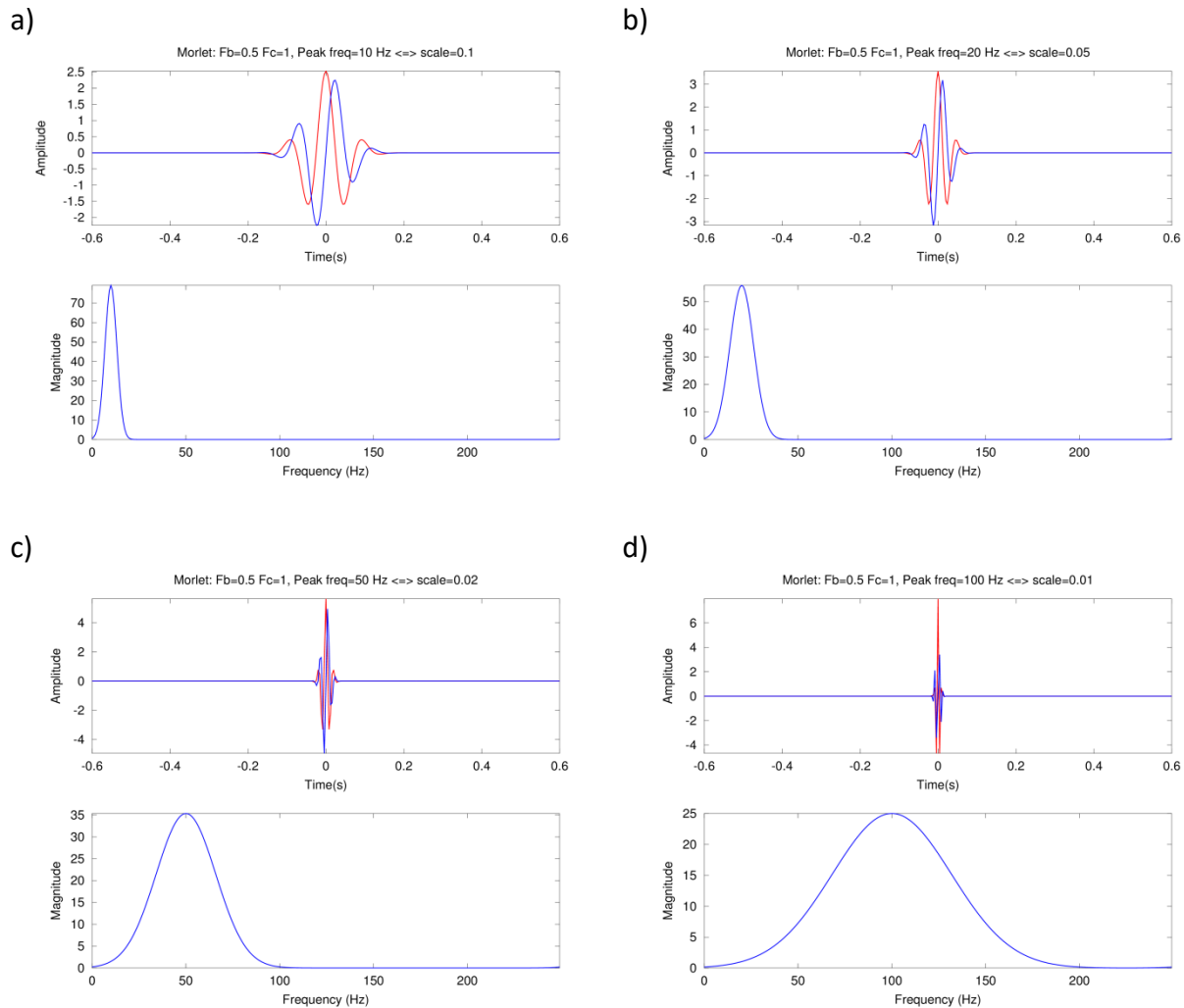


Figure 5. A suite of Morlet wavelets plotted with center frequencies (a) 10 Hz, (b) 20 Hz, (c) 50 Hz, and (d) 100 Hz. The broad band mother wavelet is defined with center frequency $f_c=1.0$ Hz and half-bandwidth $f_{B/2}=0.398$ Hz (variance $\sigma_t^2=2.0$ s²), giving rise to higher temporal resolution, but lower frequency resolution than those shown in Figure 3.

Spectral magnitude, phase, and voices

Spectral decomposition generates a suite of spectral magnitude, phase, and voice components at each time-frequency sample. Though not often used in seismic interpretation, the concept of the spectral voice provides a particularly clear means of illustrating both the mechanics and the value of spectral decomposition. The information content of voices is clearly understood when one listens to a Mozart opera, where each of the Soprano, Alto, Baritone, and Base performers often sing different words in harmony. Figure 6 shows a seismic trace, along with its time-frequency spectral magnitude, phase, and voice components. A vertical slice through the 20 Hz

Spectral Attributes: Program `spec_cwt`

spectral voice component is equivalent to applying a narrow bandpass filter centered about 20 Hz to the data.

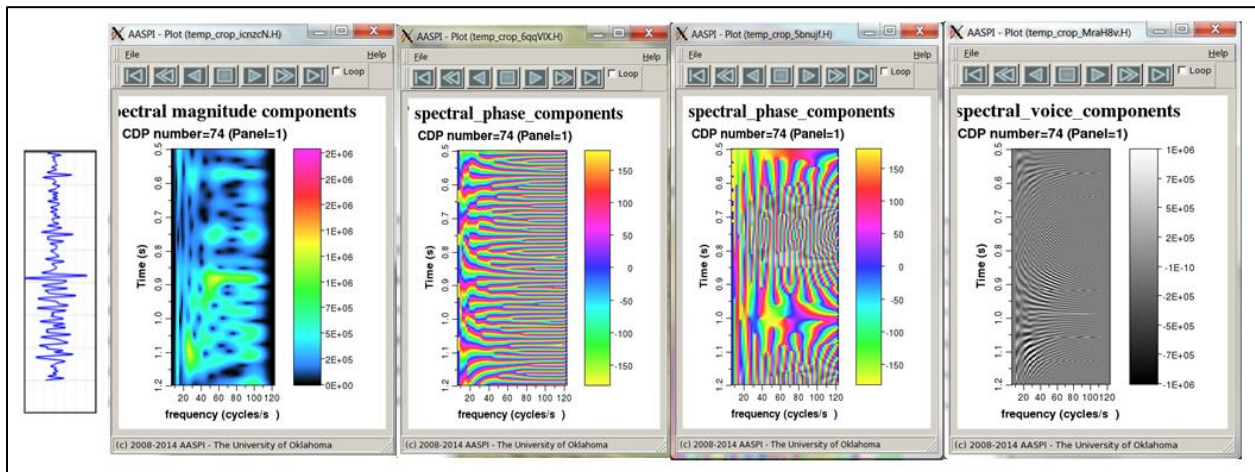
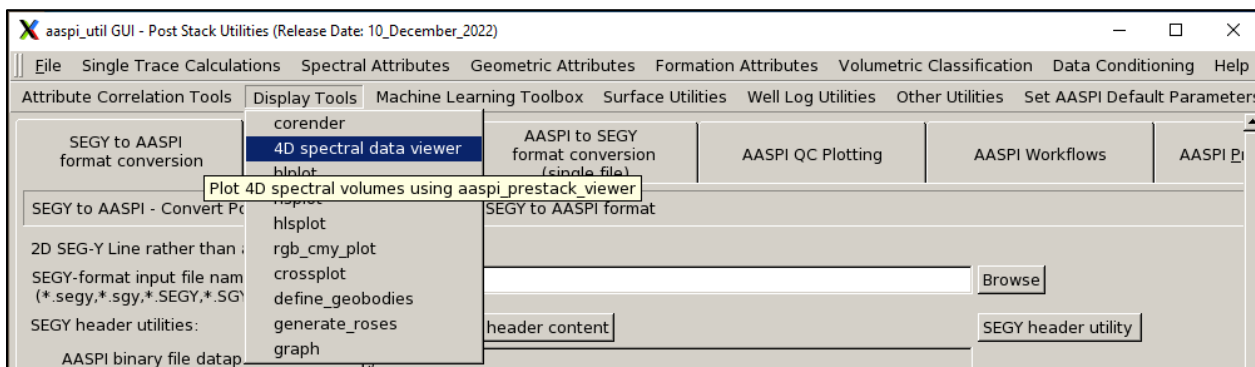


Figure 6. A representative trace showing the seismic amplitude in wiggle display, and the time frequency magnitude, phase, phase corrected for two-way travel time, and voice components. The output phase from program `spec_cwt` is corrected for the two-way travel time (i.e. the phase at each sample has been shifted by $-2\pi ft$) to better represent the phase of the reflectors rather than the distance traveled. Note the phase residues (discontinuities in phase) are readily apparent in the corrected image. The voice, $v(t,f)$, is a simple function of the magnitude, $m(t,f)$, and phase, $\phi(t,f)$, given by $v(t,f)=m(t,f)\cos[\phi(t,f)]$. The sum of the voices reconstructs the original trace, $d(t)$. Note the rapid variation in phase laterally with frequency at $t=0.8$ s. Such rapid changes require sampling with a fine frequency increment ($\Delta f=2$ Hz) in order to obtain accurate estimates of the phase residue.

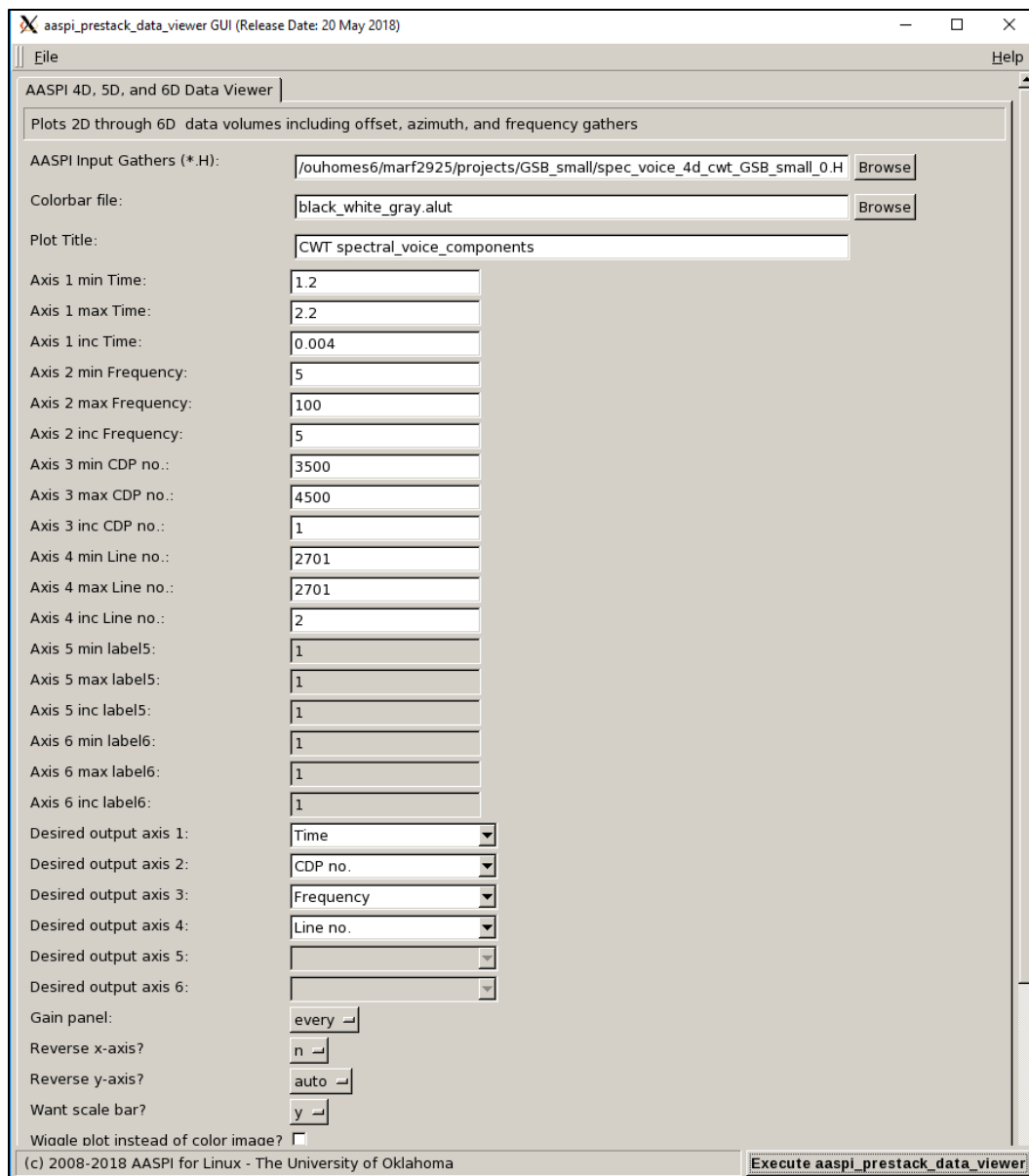
Displaying 4D (t,f,x,y) data volumes

To display 4D, 5D, or 6D spectral component hypercubes, on the `aaspi_util` menu, click *Display Tools > 4D spectral data viewer*:



The following menu appears:

Spectral Attributes: Program `spec_cwt`



In this example, I will plot the spectral magnitude file called `spec_voice_4d_cwt_GSB_small_0.H`, with the time axis running fastest, followed by the CDP no. the frequency, and finally the the Line no. axes.

Spectral Attributes: Program `spec_cwt`

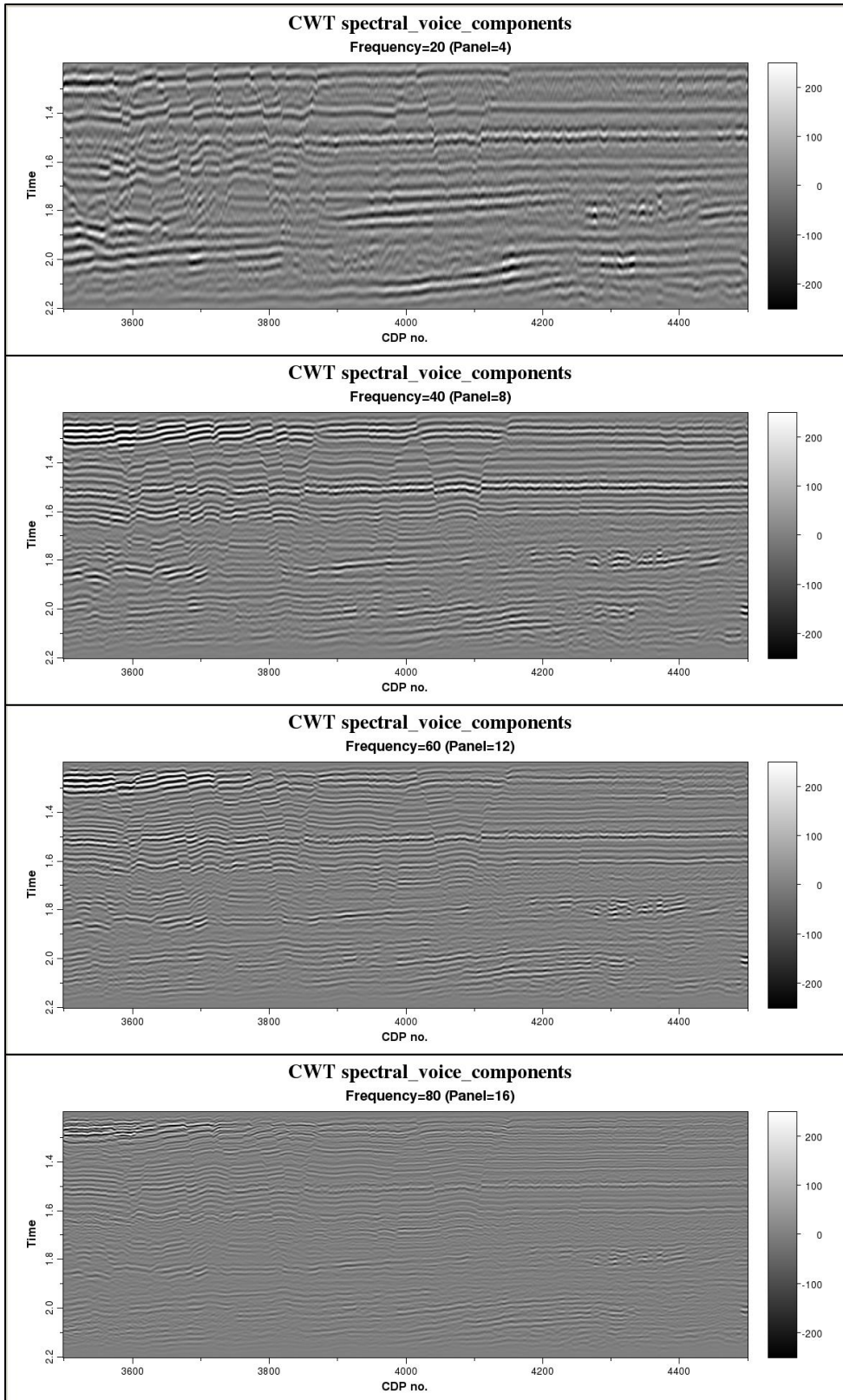


Figure 7. A suite of vertical slices through the 4D spectral voice hypercube.

Spectral Attributes: Program `spec_cwt`

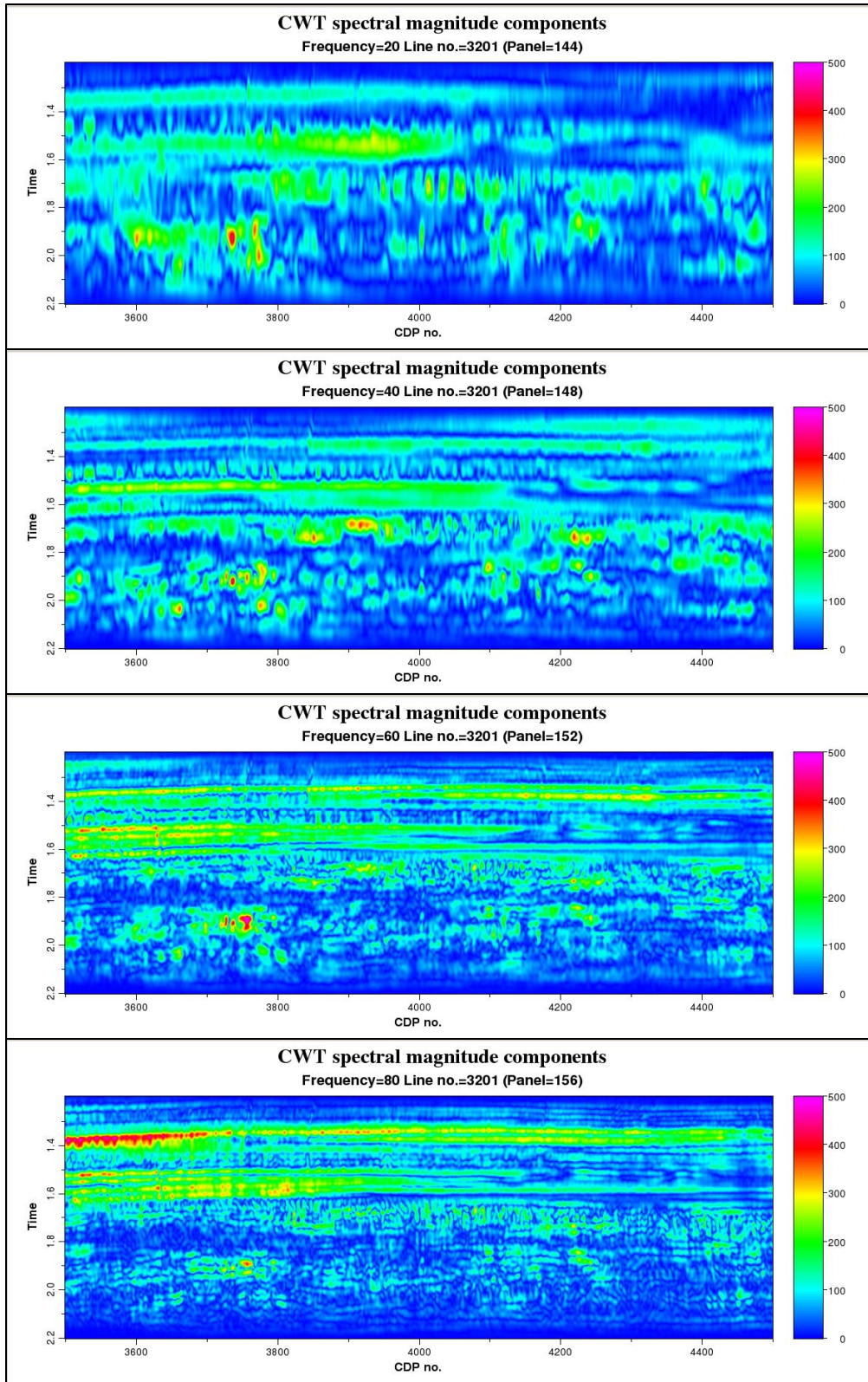


Figure 8. A suite of vertical slices through the 4D spectral magnitude hypercube.

Spectral Attributes: Program `spec_cwt`

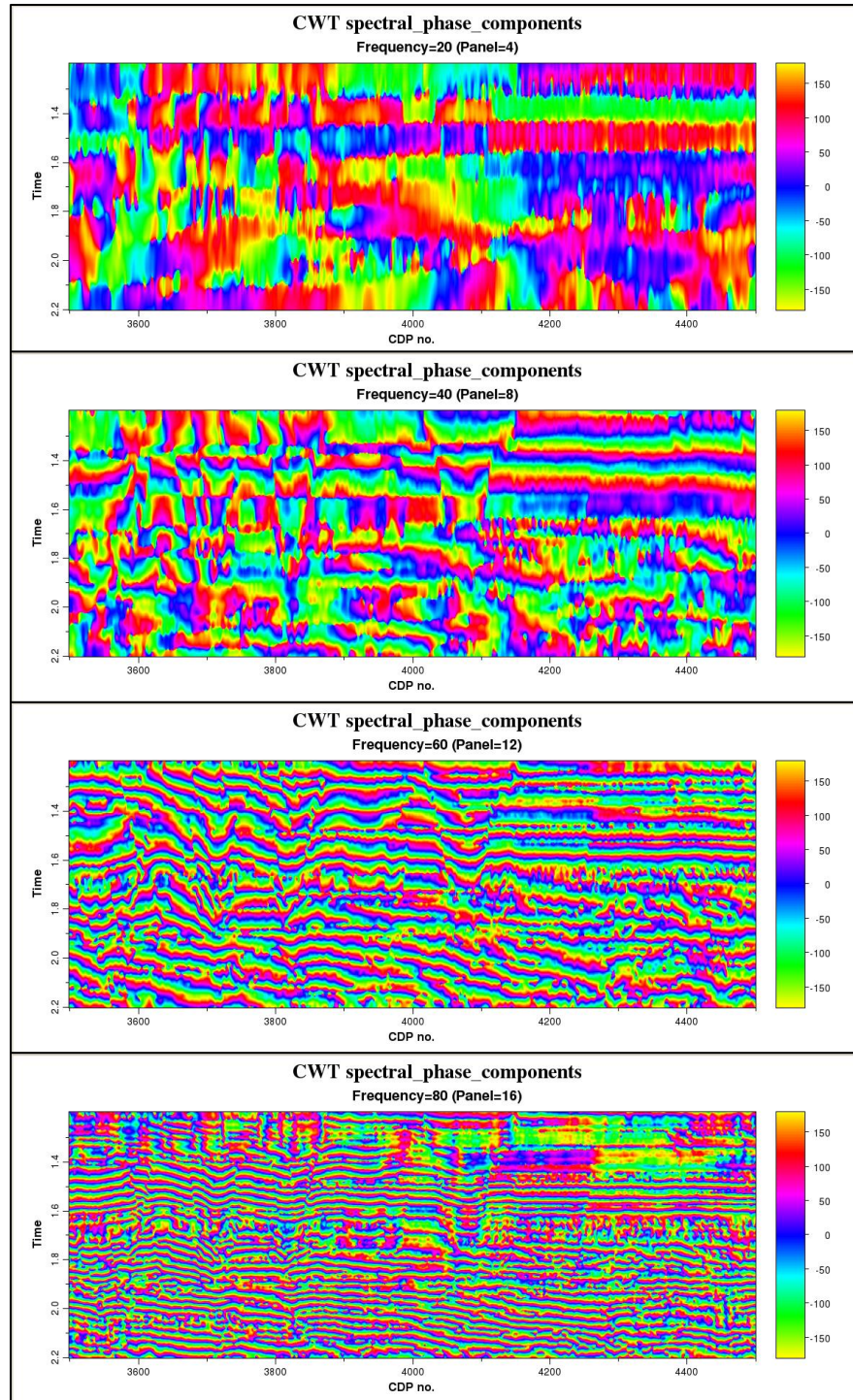


Figure 9. A suite of vertical slices through the 4D spectral phase hypercube. The phase due to the two-way traveltime $2\pi ft$ has been removed.

Spectral Attributes: Program `spec_cwt`

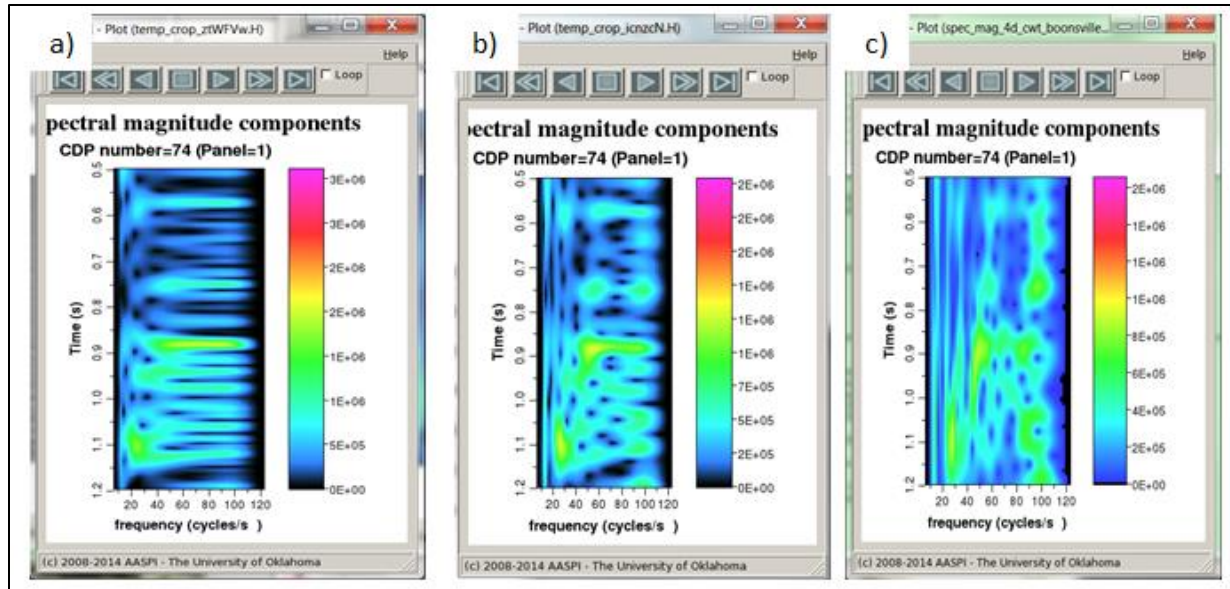
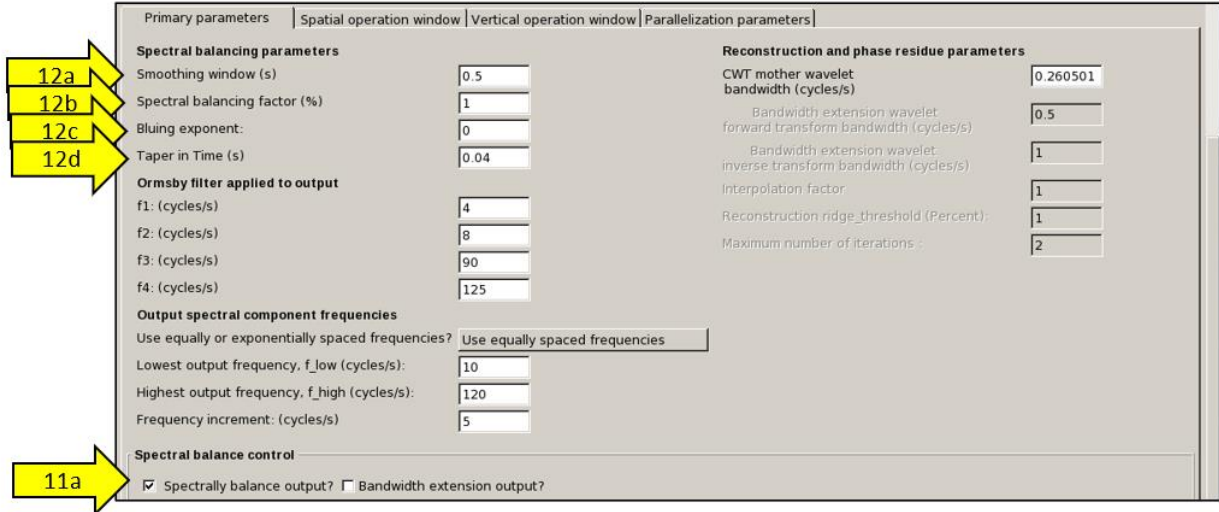


Figure 10. Spectral magnitude components for the same trace shown in the previous figure, showing the effect of the bandwidth of the mother wavelet, for half-bandwidths (a) $f_{B/2}=1.5$ Hz, (b) $f_{B/2}=1.0$ Hz, and (c) $f_{B/2}=0.67$ Hz. Note that the broader band wavelets provide greater temporal resolution, in (a) but less frequency resolution, with the magnitude varying smoothly across the frequency axis. In contrast, the narrow band wavelets in (c) provide greater frequency resolution, but less temporal resolution, with the magnitude varying more smoothly along the vertical axis. For this reason the right most narrow band choice may be better suited for spectral balancing and Q estimation, but not for interpretation of the spectral response of individual reflectors.

Spectral balancing and spectral bluing GUI parameters

Programs `spec_cmp` and `spec_cwt` are well suited for time-variant spectral balancing. At present, the average spectrum is computed for the entire survey, and then a single time-variant spectral balancing operator is applied to each trace. Trace-by-trace spectral balancing (available in program `spectral_balance`) can be dangerous, where notches in the spectra may not be statistically averaged out, such that one can remove geologic features of interest. To invoke spectral balancing and data reconstruction return the GUI and select the (11a) the *Spectrally balance output?* option and define the (12a) *Smoothing window ($K\Delta t$)*, the (12b) the *Spectral balancing parameter α* (entered as a percent), the (12c) the *Bluing exponent β* , and the (12d) *Taper* to be applied to the top and bottom of the input data to avoid Gibbs phenomena. These parameters are defined in the theory section below.

Spectral Attributes: Program `spec_cwt`



If the spectral balancing or spectral bluing options are chosen, the results are in the reconstructed data file `d_recon_unique_project_name_suffix.H`. If neither of these two options are chosen, the reconstructed data should look nearly identical to the input data so long as a sufficient range and density of frequencies have been requested.

Spectral Attributes: Program `spec_cwt`

Example 1: Spectral balancing of the Great South Basin survey

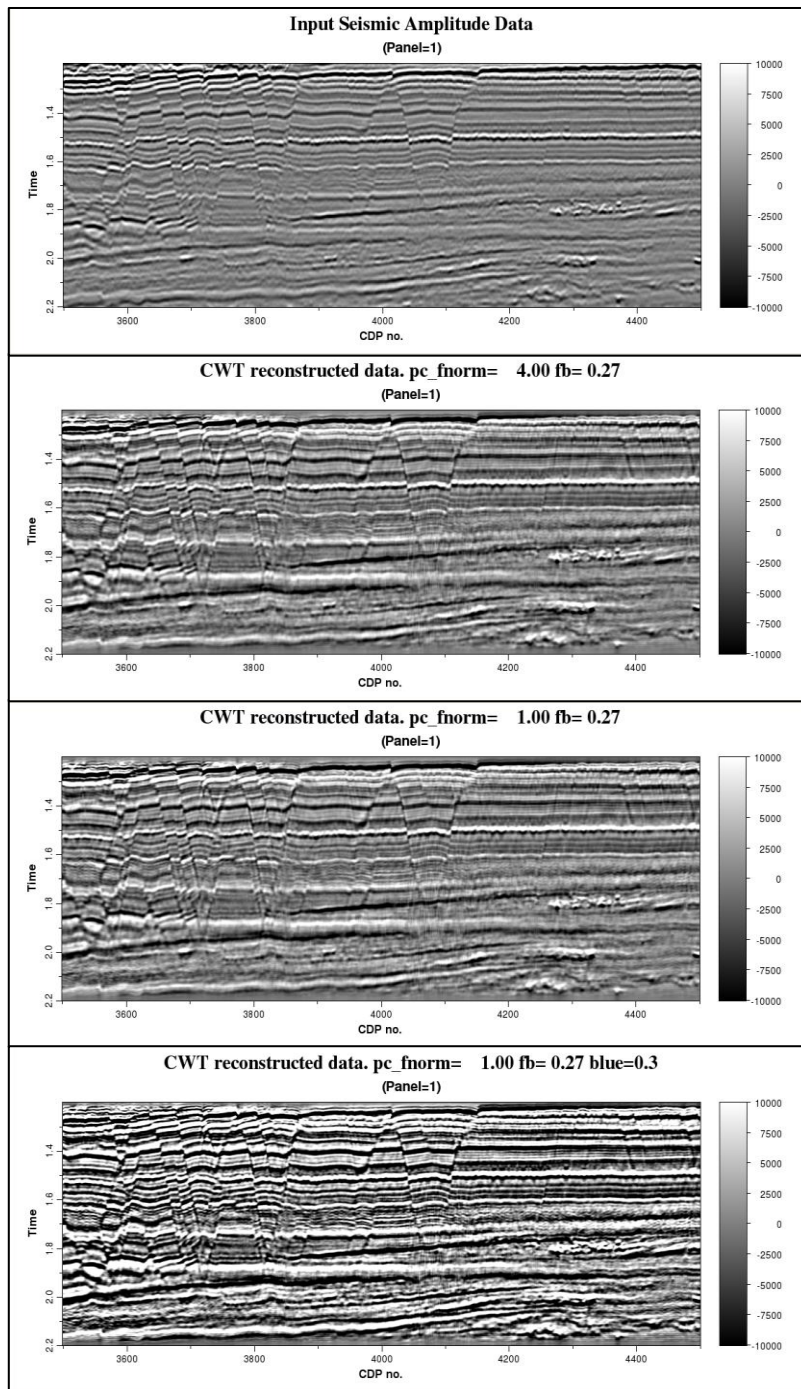


Figure 14. A suite of vertical slices at line 2701 through the (a) original data, and data after spectral balancing with a (b) $\alpha=4\%$, (c) $\alpha= 1\%$, and (d) $\alpha= 1\%$ followed by bluing with a value of $\beta=0.3$.

Spectral Attributes: Program `spec_cwt`

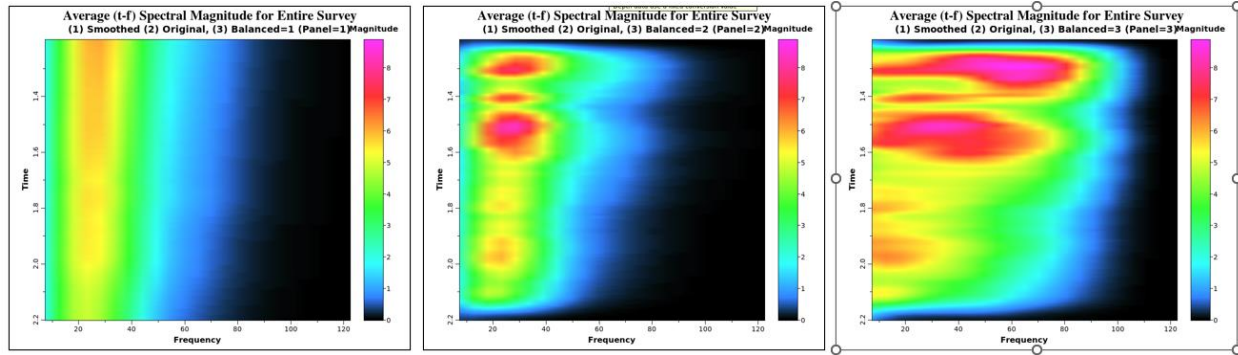


Figure 15. (Left) The vertically smoothed average magnitude spectrum. The unsmoothed average magnitude spectrum of the *GSB_small* survey (Middle) before and (Right) after spectral balancing using a factor of $\alpha=0.01$ (1 percent).

Theory: Spectral balancing and spectral bluing

Flattened spectra are obtained by balancing the power. The power of the j^{th} trace is simply the spectral magnitude squared:

$$P_j(t, f) = a_j^2(t, f). \tag{16}$$

This spectral magnitude is averaged over all traces $j=1, \dots, J$ in the survey and a $2K+1$ sample vertical analysis window to obtain the average power for each time slice t

$$P_{avg}(t, f) = \frac{1}{J(2K+1)} \sum_{k=-K}^{+K} \sum_{j=1}^J P(t+k\Delta t, f). \tag{17}$$

The peak of the average power spectrum at time t is defined as

$$P_{peak}(t) = \text{MAX}_f [P_{avg}(t, f)]. \tag{18}$$

With these definitions and a prewhitening value of $\alpha=0.01$ (1%) the flattened magnitude spectrum is computed as

$$a_j^{flat}(t, f) = \left[\frac{P_{peak}(t)}{P_{avg}(t, f) + \alpha P_{peak}(t)} \right]^{1/2} a_j(t, f). \tag{19}$$

Traditionally, the goal of seismic processing was to produce a flat spectrum. However, Neep (2007) and others built on earlier “colored inversion” work that showed the reflectivity spectrum derived from good logs behaves as f^β where $0.0 < \beta < 0.4$. The more general spectral bluing filter is then

$$a_j^{blue}(t, f) = \left[\frac{P_{peak}(t)}{P_{avg}(t, f) + \alpha P_{peak}(t)} \right]^{1/2} f^\beta a_j(t, f) \tag{20}$$

Statistical measures of the spectra

If time and disk space permit, the interpreter should animate through all the magnitude and phase spectral components, using pattern recognition to identify depositional, diagenetic, or structural patterns of interest. Although such animation is possible when restricted to one or two geologic formations, for very large 3D surveys there are too many volumes to use as a data-scoping tool. The second approach is to corender three key components using RGB, using commercial software or AASPI program **corender**. Modern interpretation software allows the interpreter to interactively adjust components to determine an optimum combination.

An alternative to color blending is to compute statistical measures of the spectrum. Taner et al.’s (1979) instantaneous attributes provide a measure of the average frequency and bandwidth for

Spectral Attributes: Program **spec_cwt**

isolated Morlet or Ricker wavelets. If the power spectrum is Gaussian with a mean of μ and standard deviation σ , the average frequency and the peak frequency are both μ , the bandwidth is 2σ , the skewness is 0, and the kurtosis is 0. However, almost all seismic data have been spectrally balanced in the processing shop prior to loading onto the interpretation workstation. Further spectral balancing can be applied using AASPI programs **spec_cwt**, **spec_cmp**, and **spectral_balance** to minimize the effect of the source wavelet, such that the Gaussian approximation is inappropriate. For that reason, Zhang et al. (2008) proposed a suite of statistical measures based on the histogram of the spectrum at each voxel which we modify here.

Theory: Statistical measures of the spectra (peak frequency, peak magnitude, and bandwidth)

The peak spectral frequency and peak spectral magnitude

The mode is one of the simplest statistical measures and can often be directly related to thin-bed tuning (Figure A3), where the tuning thickness in two-way traveltime, $T_{\text{tuning}} = 1/(2 * f_{\text{peak}})$. If the spectrum at J discrete frequency samples, the peak frequency f_{peak} is defined as

$$f_{\text{peak}} = b_1 f_{j_{\text{peak}}-1} + b_2 f_{j_{\text{peak}}} + b_3 f_{j_{\text{peak}}+1}, \quad (17)$$

where

$$j_{\text{peak}} = \text{MIN} \left\{ \text{ARG} \left[\frac{1}{2} a(f_{\text{peak}}) \right] \right\}, \quad (21)$$

and where b_1 , b_2 , and b_3 are interpolation weights obtained by fitting a parabola through the values $f_{j_{\text{peak}}-1}$, $f_{j_{\text{peak}}}$, and $f_{j_{\text{peak}}+1}$.

The same parabola provides the magnitude at the peak frequency:

$$a_{\text{peak}} \equiv a(f_{\text{peak}}) = c_1 a(f_{j_{\text{peak}}-1}) + c_2 a(f_{j_{\text{peak}}}) + c_3 a(f_{j_{\text{peak}}+1}). \quad (22)$$

The spectral bandwidth

In physical acoustics, the bandwidth is defined as the frequency distance between the lowest and highest half-magnitude frequency components

$b \equiv f_{\text{high}}^{(1/2)} - f_{\text{low}}^{(1/2)}$, where

$$a(f_{\text{low}}^{(1/2)}) \equiv \text{MIN}_f \left[\frac{1}{2} a(f_{\text{peak}}) \right], \text{ and} \quad (23)$$

$$a(f_{\text{high}}^{(1/2)}) \equiv \text{MAX}_f \left[\frac{1}{2} a(f_{\text{peak}}) \right].$$

The mean spectral magnitude and the mean spectral frequency

The mean spectral magnitude is simply

$$a_{\text{mean}} \equiv \frac{1}{J} \sum_{j=1}^J a(f_j). \quad (24)$$

and mean frequency is

$$f_{\text{mean}} \equiv \frac{\sum_{j=1}^J a(f_j) f_j}{\sum_{j=1}^J a(f_j)}. \quad (25)$$

The peak spectral magnitude above the mean

Stronger events will have a stronger peak magnitude. To better estimate how strongly an event is tuned we can compute the peak spectral magnitude above the mean:

$$a_{\text{peak_above_mean}} \equiv a_{\text{peak}} - a_{\text{mean}}$$

Theory: Statistical measures of the spectra (effective kurtosis and skewness)*Spectral kurtosis and effective kurtosis*

Kurtosis is computed from the fourth moment of the spectra

$$k \equiv \frac{\sum_{j=1}^J [a(f_j)f_j - f_{\text{mean}}]^4}{\left\{ \sum_{j=1}^J [a(f_j)f_j - f_{\text{mean}}]^2 \right\}^2} \quad (27)$$

In statistics, a thin-tailed platykurtic distribution has truncated or shorter tails than a Gaussian, with values of $k < 3$. A medium-tailed mesokurtic distribution has similar tails to a Gaussian distribution which has a value of $k = 3$. Finally, a thick-tailed leptokurtic distribution has longer tails than a Gaussian and has values of $k > 3$. For this reason, a more useful measure is the effective kurtosis

$$k_{\text{eff}} \equiv k - 3 = \frac{\sum_{j=1}^J [a(f_j)f_j - f_{\text{mean}}]^4}{\left\{ \sum_{j=1}^J [a(f_j)f_j - f_{\text{mean}}]^2 \right\}^2} - 3, \quad (28)$$

where a Gaussian distribution has $k_{\text{eff}} \approx 0$, a thin-tailed platykurtic distribution has $k_{\text{eff}} < 0$, and a thick-tailed leptokurtic distribution has $k_{\text{eff}} > 0$.

Spectral skewness

Skewness is computed from the third moment of the spectra and measures whether the distribution is asymmetric about the mean value:

$$s \equiv \frac{\sum_{j=1}^J [a(f_j)f_j - f_{\text{mean}}]^3}{\left\{ \sum_{j=1}^J [a(f_j)f_j - f_{\text{mean}}]^2 \right\}^{3/2}} \quad (29)$$

In statistics, a distribution with $s = 0$ (such as a Gaussian distribution) is symmetric about the mean. Distributions that are skewed towards higher values have $s > 0$, whereas distributions that are skewed towards lower values have $s < 0$.

Spectral response of common impedance changes*Spectral response of a discrete jump in impedance*

If the impedance in a shallower layer is Z_1 and the impedance in a deeper layer is Z_2 , the reflection coefficient is

$$R(t) = \frac{Z_2 - Z_1}{Z_2 + Z_1} f^0. \quad (30)$$

where I have added the last term to show that there is no change in frequency. The change in phase is 0° for $R(t) > 0$ and 180° for $R(t) < 0$.

Seismic response of a thin bed embedded in a constant impedance matrix

For a thin bed of constant impedance Z_2 and thickness T embedded in a matrix of impedance Z_1 , the reflected wave has the form

$$u(t) = \left\{ \frac{Z_2 - Z_1}{Z_2 + Z_1} \exp \left[+i2\pi f \frac{T}{2} \right] - \frac{Z_1 - Z_2}{Z_1 + Z_2} \exp \left[-i2\pi f \frac{T}{2} \right] \right\}. \quad (31)$$

Using Euler's formula

$$\exp(i\theta) = \cos \theta + i \sin \theta, \quad (32)$$

such that

$$\exp(i\theta) - \exp(-i\theta) = 2i \sin \theta, \quad (33)$$

equation 3 becomes

$$u(t) = \frac{Z_2 - Z_1}{Z_2 + Z_1} \left\{ \exp \left[+i\pi f \frac{T}{2} \right] - \exp \left[-i\pi f \frac{T}{2} \right] \right\} = \frac{Z_2 - Z_1}{Z_2 + Z_1} 2i \sin(\pi f T) \quad (34)$$

Allowing T to approach zero gives

$$\lim_{T \rightarrow 0} u(t) = \lim_{T \rightarrow 0} \frac{Z_2 - Z_1}{Z_2 + Z_1} 2i \sin(\pi f T) = i2\pi f \Delta T \frac{Z_2 - Z_1}{Z_2 + Z_1}, \quad (35)$$

such that spectral response of a thin bed increases as f^{+1} . There is also a 90° phase change.

Seismic response of a thin bed embedded in an increasing impedance matrix

Let's now assume the same geometry as the previous example, but now with an upper medium Z_1 , embedded layer Z_2 , and lower medium Z_3 , where $Z_3 - Z_2 = Z_2 - Z_1 = \Delta Z$. (i.e. the change in impedance is the same giving rise to nearly identical reflection coefficients $r(t)$). In this case, the reflected wavefield has the form

$$u(t) = r(t) \left\{ \exp \left[+i2\pi f \frac{T}{2} \right] + \exp \left[-i2\pi f \frac{T}{2} \right] \right\} = 2r(t) \cos(\pi f T). \quad (36)$$

Letting T approach zero gives

$$\lim_{T \rightarrow 0} R(t) = 2r(t) = \frac{Z_3 - Z_1}{Z_3 + Z_1} f^0, \quad (37)$$

such that there is no spectral change with frequency and a phase change of either a 0° for $R(t) > 0$ and 180° for $R(t) < 0$.

Spectral Attributes: Program `spec_cwt`

Spectral response of a linear increase or decrease in impedance

If the impedance increases linearly within a layer and has the form

$$Z(t) = \alpha + \beta t, \quad (41)$$

where t denotes the two-way travel time, then the reflection coefficient has the form

$$R(t) = \frac{Z(t + \delta t / 2) - Z(t - \delta t / 2)}{Z(t + \delta t / 2) + Z(t - \delta t / 2)} = \frac{\beta \delta t}{2\alpha}. \quad (42)$$

For an incident wave of the form $\exp(-i2\pi ft)$ the reflection response to such a linear increase in impedance is

$$u(t) = \sum R(t) \exp(i2\pi ft) = \int \frac{\beta}{2\alpha} \exp(i2\pi ft) \delta t = \frac{\beta \exp(i2\pi ft)}{\alpha i 4\pi f}, \quad (43)$$

Or at time $t=0$, the reflection coefficient from the ramp is

$$R(t) = \frac{-i\beta}{\alpha 4\pi f}, \quad (44)$$

such that the spectral response decreases with frequency as f^{-1} with a $\pm 90^\circ$ phase shift depending on the sign of β .

Thus, for a simple ramp, the reflection response acts as a simple integration, increasing the low frequency content and rotating the response by $\pm 90^\circ$ depending on the sign of β .

Seismic response of a finite ramp of thickness ΔT

For a ramp of finite thickness, we need to account for two endpoints. Let's center the ramp of thickness T about the origin $t=0$:

$$\begin{aligned} u(t) &= \frac{\beta}{2\alpha} \int_{-T/2}^{+T/2} \exp(i2\pi ft) \delta t = \frac{\beta \exp(i2\pi ft)}{\alpha i 4\pi f} \Bigg|_{-T/2}^{+T/2} \\ &= \frac{\beta}{\alpha i 4\pi f} \left\{ \exp\left[i2\pi f \frac{T}{2}\right] - \exp\left[-i2\pi f \frac{T}{2}\right] \right\} = \frac{\beta}{\alpha 2\pi f} \sin(\pi f T) \end{aligned} \quad (45)$$

Let's assume that the value of the impedances given by equation the top and bottom of the ramp are defined by

$$Z(-\Delta T / 2) = \alpha - \beta \Delta T / 2 = Z_1, \quad (47a)$$

and

$$Z(+\Delta T / 2) = \alpha + \beta \Delta T / 2 = Z_2, \quad (47b)$$

such that

$$\beta = \frac{Z_2 - Z_1}{\Delta T}. \quad (48a)$$

and

$$\alpha = \frac{Z_2 + Z_1}{2}. \quad (48b)$$

Inserting equations 8a and 8b into equation 6 and allowing T to approach zero gives

$$\lim_{\Delta T \rightarrow 0} u(t) = \lim_{\Delta T \rightarrow 0} \frac{\beta}{\alpha 2\pi f} \sin[\pi f \Delta T] = \frac{\beta}{\alpha 2\pi f} \pi f \Delta T = \frac{\beta \Delta T}{2\alpha} = \frac{Z_2 - Z_1}{Z_2 + Z_1}, \quad (49)$$

which is the correct reflection coefficient for a discrete jump in impedance.

Theory: Statistical measures of the spectra (Logarithmic slope and roughness)

For very thin Type I reflectivity layering, the first tuning peak occurs beyond the value of f_3 in the balanced spectrum, such that the spectral magnitude increases linearly between f_2 and f_3 . For linear impedance gradients that in certain cases may be associated with upward fining and upward coarsening sedimentation, the spectrum varies inversely with the frequency between f_2 and f_3 . A simple jump in impedance gives no change in the spectrum between f_2 and f_3 . These end members can be measured by computing the slope of the logarithm of the magnitude spectrum against the logarithm of the frequency. The logarithmic slope is closely related to the Hölder (also called the Lipschitz) exponent described by Li and Liner (2004). Defining j_2 and j_3 as the indices of the discrete frequencies f_2 and f_3 , we simply minimize the error e_j :

$$e_j = (m \log f_j + c) - \log [a(f_j)]$$

where m is the unknown logarithmic slope and c is an unknown constant. To do so, we define the weighted normal equations

$$\mathbf{W}\mathbf{A}\mathbf{x} = \mathbf{W}\mathbf{b} \tag{50}$$

where the matrix

$$\mathbf{A} = \begin{bmatrix} \log(f_{j_2}) & \log(f_{j_2+1}) & \cdots & \log(f_{j_3}) \\ 1 & 1 & \cdots & 1 \end{bmatrix}^T, \tag{51}$$

the unknown vector

$$\mathbf{x} = [m \quad c]^T, \tag{52}$$

and the right-hand side is

$$\mathbf{b} = \left\{ \log [a(f_{j_2})] \quad \log [a(f_{j_2+1})] \quad \cdots \quad \log [a(f_{j_3})] \right\}^T. \tag{53}$$

In general, the data will have been spectrally balanced, with the average spectrum of the survey denoted as $\bar{a}(t, f)$ at time t . In order to make the spectrum flatter (but noisier) than provided by spectral balancing, we redefine the values of $a(f_j)$ to be $a(f_j) / \bar{a}(t, f_j)$. Because we have less confidence in these rescaled values, we weight them by a diagonal matrix

$$W_{jk} = \begin{cases} \bar{a}(t, f_j) & \text{if } k = j \\ 0 & \text{if } k \neq j \end{cases} \tag{54}$$

The standard weighted least-squares solution is to form the normal equations by multiplying both sides of equation 50 by the transpose of $\mathbf{W}\mathbf{A}$ which is $\mathbf{A}^T\mathbf{W}^T$

$$\mathbf{A}^T\mathbf{W}^T\mathbf{W}\mathbf{A}\mathbf{x} = \mathbf{A}^T\mathbf{W}^T\mathbf{W}\mathbf{b}. \tag{55}$$

Inverting the (now square 2x2) matrix gives

$$\mathbf{x} = (\mathbf{A}^T\mathbf{W}^T\mathbf{W}\mathbf{A})^{-1} \mathbf{A}^T\mathbf{W}^T\mathbf{W}\mathbf{b}. \tag{56}$$

Spectral roughness

The error between this linear estimate and the measured spectral ratios is given by

$$\mathbf{e} = \mathbf{W}[\mathbf{A}\mathbf{x} - \mathbf{b}], \tag{57}$$

Providing an estimate of roughness of how well the linear model fits the data:

$$r = \frac{\mathbf{e}^T\mathbf{e}}{\mathbf{b}^T\mathbf{W}^T\mathbf{W}\mathbf{b}}. \tag{58}$$

which will range in value between 1 (a very poor fit) and 0 (a perfect fit).

Example 2: Statistical Measures of the spectra (Great South Basin survey)

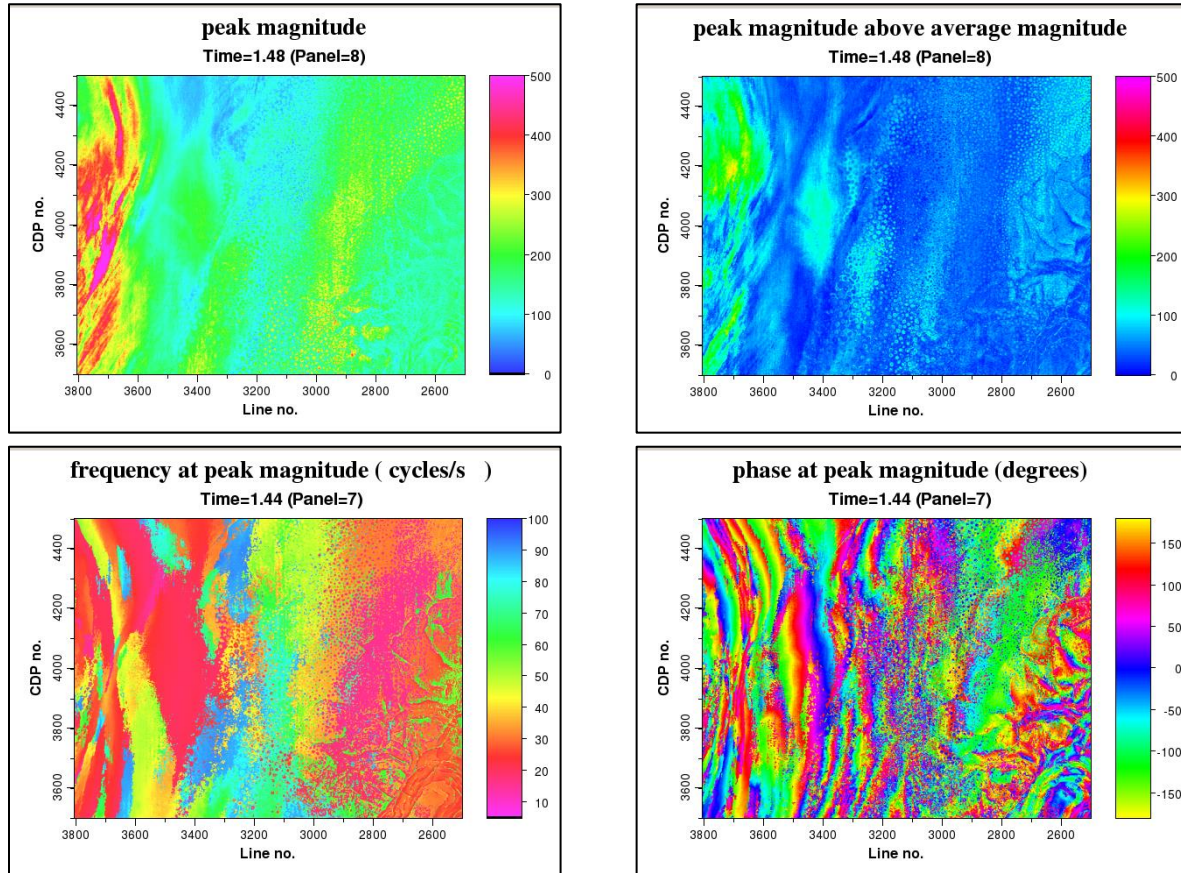


Figure 11. The results obtained when selecting the *Want peak attributes* option for the *GSB_small* survey. Times slices at $t=1.48$ s through (upper left) peak magnitude, (upper right) peak magnitude above the average magnitude, (lower left) peak frequency, and (lower right) peak phase. If the data has been spectrally balanced, the peak frequency provides an excellent estimate of the tuning frequency, and hence the layer thickness.

Spectral Attributes: Program `spec_cwt`

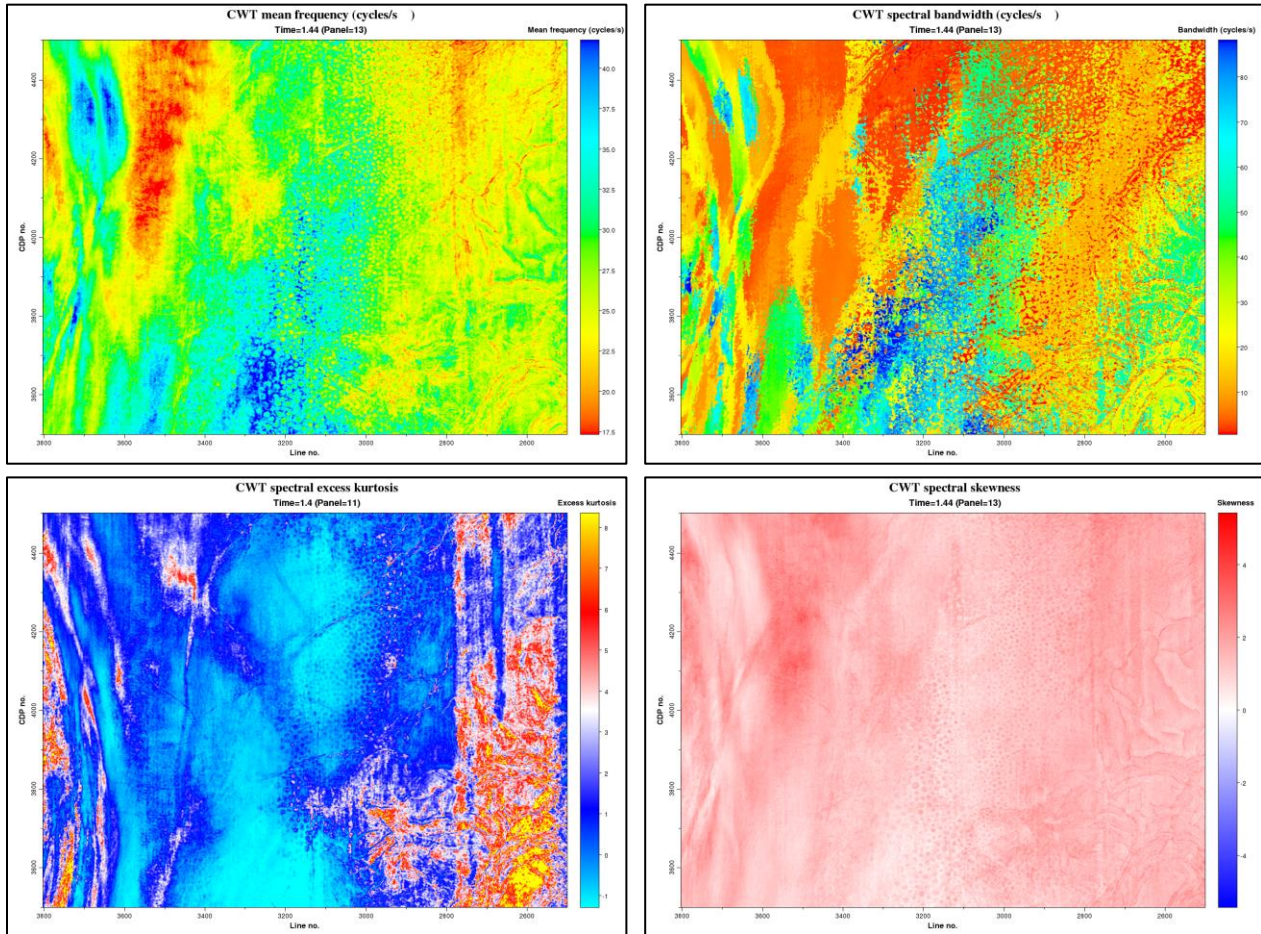


Figure 12. The results obtained when selecting the *Want spectral bandwidth and mean frequency* and *Want spectral slope and roughness* and *Want spectral excess kurtosis and skewness* options for the *GSB_small* survey. Times slices through (upper left) mean frequency, (upper right) bandwidth, (lower left) excess kurtosis, and (lower right) skewness. Spectral bandwidth and mean frequency are often good for facies definition. Spectral kurtosis and skewness are sometimes used to estimate Q between two picked horizons.

Spectral Attributes: Program `spec_cwt`

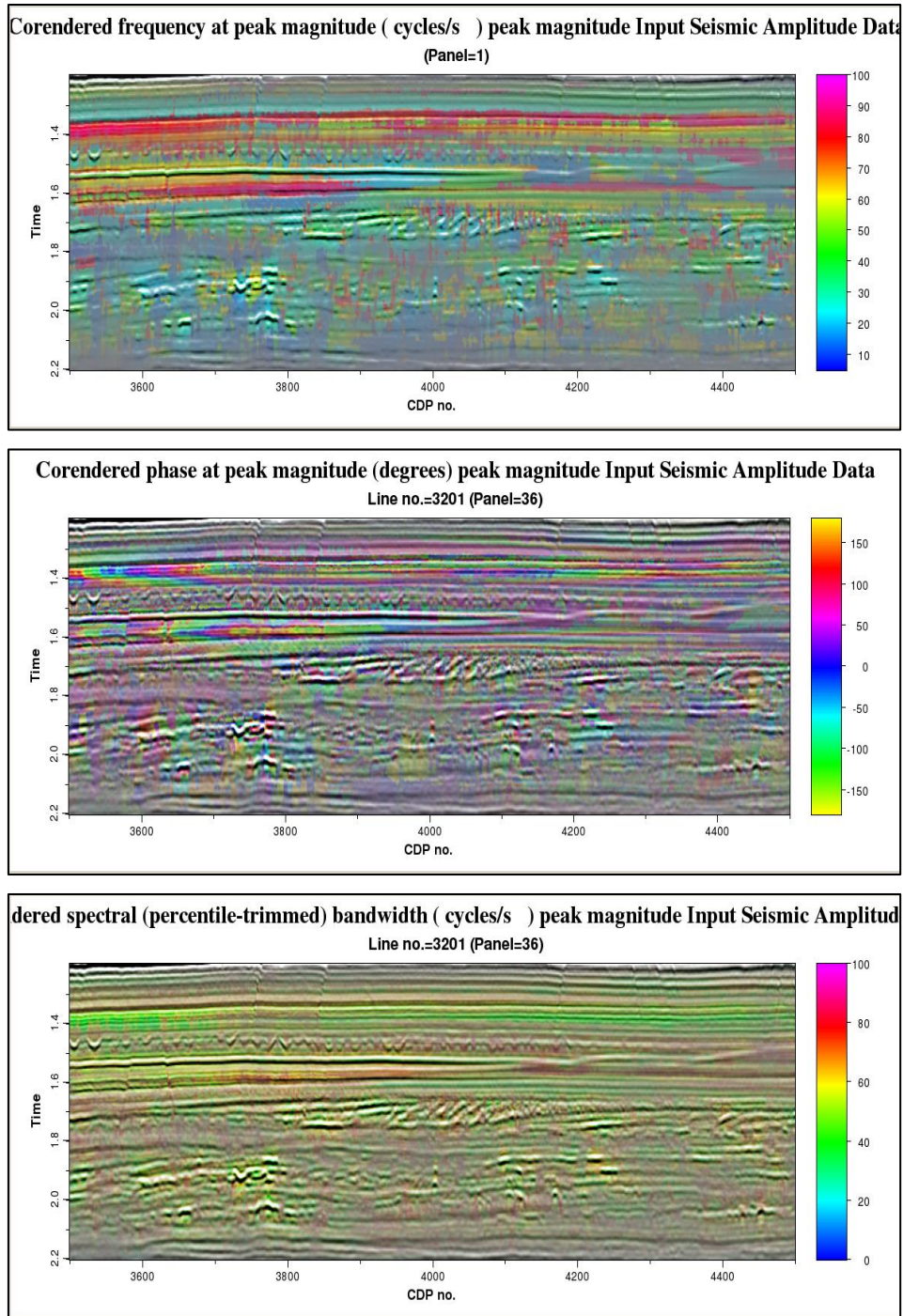


Figure 13. Representative vertical slices obtained when selecting the *Want peak attributes* and *Want spectral bandwidth and mean frequency* options for the *GSB_small survey*, in this case corendered with seismic amplitude using a binary black-white color bar using AASPI program `corender`. (Top) Peak frequency plotted against a polychromatic frequency color bar corendered with peak magnitude plotted against a monochrome gray color bar. (Middle) Peak phase plotted against a polychromatic cyclic color bar corendered with peak magnitude plotted against a monochrome gray color bar. (Bottom) Bandwidth plotted against a polychromatic frequency color bar corendered with peak magnitude plotted against a monochrome gray color bar.

Spectral Attributes: Program `spec_cwt`

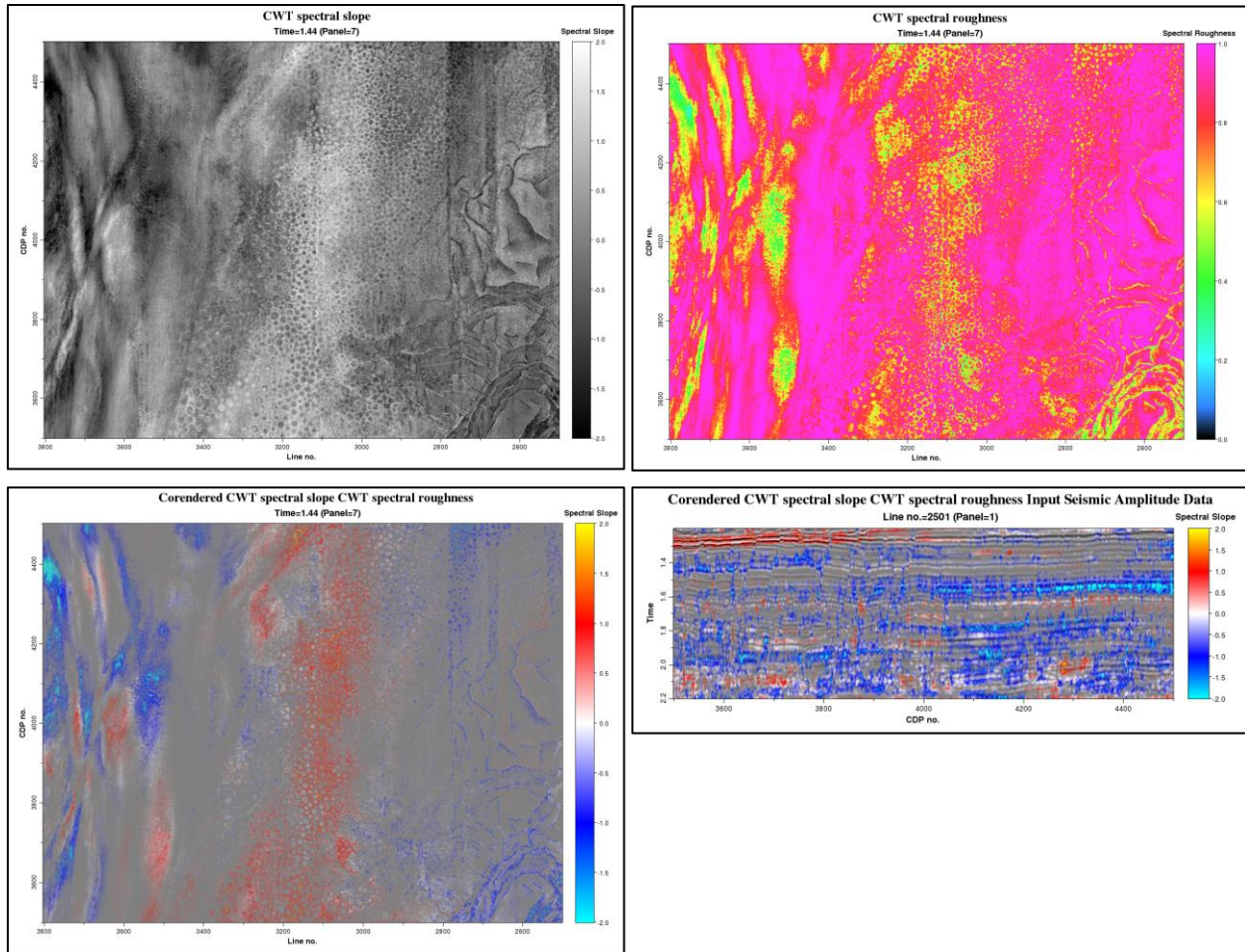


Figure 14. (Top) Time slices through the logarithmic spectral slope and spectral roughness volumes. Note that in most areas the linear $\text{LOG}(\text{mag})\text{-LOG}(\text{freq})$ model is poor, resulting in high values of roughness. (Lower Left) Corendered logarithmic spectral slope (plotted against a dual polarity yellow-red-white-blue-cyan colorbar) and spectral roughness (plotted against a monochrome gray color bar with transparent values at $r=0$ and opaque values at $r=1$). (Lower right) A vertical slice showing corendered logarithmic spectral slope, spectral roughness, and seismic amplitude. Areas that are gray are poorly represented by the linear $\text{LOG}(\text{mag})\text{-LOG}(\text{freq})$ model.

Limiting the zone of application

There are two reasons to limit the zone of application. The first is simply to limit the amount of output when requesting multiple spectral components by limiting the time window of application. The second is for parameter testing, such as the percentage of spectral balancing or bluing to use. There are two tabs that control the amount of output – the first defines the *Spatial Operation Window* while the second defines the *Temporal Operation Window*. The definition of the spatial operation window is similar to many other AASPI applications. In this example, the input is a stacked 3D migrated data volume, such that are three axes – time, CDP no., and Line no.

Spectral Attributes: Program `spec_cwt`

Primary parameters	Spatial Operation Window	Temporal Operation Window	Parallelization parameters
Min CDP no.:	<input type="text" value="950"/>		
Max CDP no.:	<input type="text" value="2950"/>		
Min Line no.:	<input type="text" value="3650"/>		
Max Line no.:	<input type="text" value="4470"/>		
Min :	<input type="text" value="1"/>		
Max :	<input type="text" value="1"/>		
Min :	<input type="text" value="1"/>		
Max :	<input type="text" value="1"/>		
Number of traces in memory on master for synchronization:	<input type="text" value="1000"/>		
Maximum memory on master in Gbytes:	<input type="text" value="2"/>		

If the input is a suite of prestack-migrated gathers, the grayed-out boxes provide a means of limiting the range of azimuths and offsets processed. Simply define the range of CDPs and lines that you desire to process.

Primary parameters	Spatial Operation Window	Temporal Operation Window	Parallelization parameters
Help - Horizon Definition			
Fixed time window?:	<input checked="" type="radio"/>		
Compute about and between two horizons?:	<input type="radio"/>		
Compute about a single flattened horizon?:	<input type="radio"/>		
Start Time in s:	<input type="text" value="1.5"/>		
End Time in s:	<input type="text" value="2.5"/>		
Input shallower horizon filename:	<input type="text"/>	<input type="button" value="Browse"/>	
(Choose Horizon Type Below:)		<input type="button" value="View horizon file"/>	<input type="button" value="Convert DOS to Unix"/>
Window start wrt shallower horizon in s (vertical axis positive down):	<input type="text" value="-0.1"/>		
Input deeper horizon filename:	<input type="text"/>	<input type="button" value="Browse"/>	
(Choose Horizon Type Below:)		<input type="button" value="View horizon file"/>	<input type="button" value="Convert DOS to Unix"/>
Window start wrt deeper horizon in s (vertical axis positive down):	<input type="text" value="0.1"/>		
Choose horizon type:	<input type="text" value="gridded (e.g. EarthVision)"/>		
Number of header lines to skip:	<input type="text" value="0"/>		
Total number of columns:	<input type="text" value="5"/>		
Column number of line_no:	<input type="text" value="1"/>		
Column number of cdp_no:	<input type="text" value="2"/>		
Column number of time or depth picks:	<input type="text" value="5"/>		
znull value (indicates missing pick):	<input type="text" value="-999999"/>		
Vertical axis of picked surface?	<input type="text" value="Positive Down"/>		
Vertical Units of Picked Horizons:	<input type="text" value="ms"/>		

In this first example, we click the *Fixed time window?* button, which grays out all of the other boxes except the *Start time in s* and *End time in s* areas. This option is common to many other

Spectral Attributes: Program `spec_cwt`

AASPI programs, where the default is the complete range of the input data volume to be analyzed.

If we click the *Compute about and between two horizons?* button, the previous two options are grayed out.

The screenshot shows the 'spec_cwt' program interface with the 'Temporal Operation Window' tab selected. The 'Compute about and between two horizons?' radio button is selected, while 'Fixed time window?' and 'Compute about a single flattened horizon?' are unselected and grayed out. The interface includes the following fields and controls:

- Fixed time window?:
- Compute about and between two horizons?:
- Compute about a single flattened horizon?:
- Start Time in s:
- End Time in s:
- Input shallower horizon filename:
- (Choose horizon type below):
- Window start wrt shallower horizon in s (vertical axis positive down):
- Input deeper horizon filename:
- (Choose horizon type below):
- Window start wrt deeper horizon in s (vertical axis positive down):
- Choose horizon type:
- Number of header lines to skip:
- Total number of columns:
- Column number of line_no:
- Column number of cdp_no:
- Column number of time or depth picks:
- znull value (indicates missing pick):
- Vertical axis of picked surface?
- Vertical Units of Picked Horizons:

We are now prompted to add an upper and lower horizon file name as well as a relative start and end time to those two horizons. At present, there are two horizon formats supported, a gridded (as in x, y control points or “knots” defining a B-spline map) EarthVision format, and an interpolated format (such as from Kingdom Suite and SeisX where each trace has a corresponding picked time). More formats are possible, but you will need to send us a definition of the format. Selecting the *Compute about a single flattened horizon* button requires only a single horizon and a window of relative start and end times about it. As you can see below, the 2nd horizon is set to be equivalent to the (previously upper) single horizon and is grayed out:

Spectral Attributes: Program `spec_cwt`

Primary parameters | Spatial Operation Window | Temporal Operation Window | Parallelization parameters | [Help - Horizon Definition](#)

Fixed time window?:

Compute about and between two horizons?:

Compute about a single flattened horizon?:

Start Time in s:

End Time in s:

Input single horizon filename:

(Choose horizon type below:)

Window start wrt the single horizon in s (vertical axis positive down):

No second horizon needed:

(Choose horizon type below:)

Window start wrt the single horizon in s (vertical axis positive down):

Choose horizon type:

Number of header lines to skip:

Total number of columns:

Column number of line_no:

Column number of cdp_no:

Column number of time or depth picks:

znnull value (indicates missing pick):

Vertical axis of picked surface?

Vertical Units of Picked Horizons:

More detailed discussion on the *Temporal Operation Window* tab can be found under its own *Help – Horizon Definition* tab.

The output computed between two fixed time levels is easy to understand. In this example, I constructed the spectrally balanced output to fall between 1.5 s and 2.5 s:

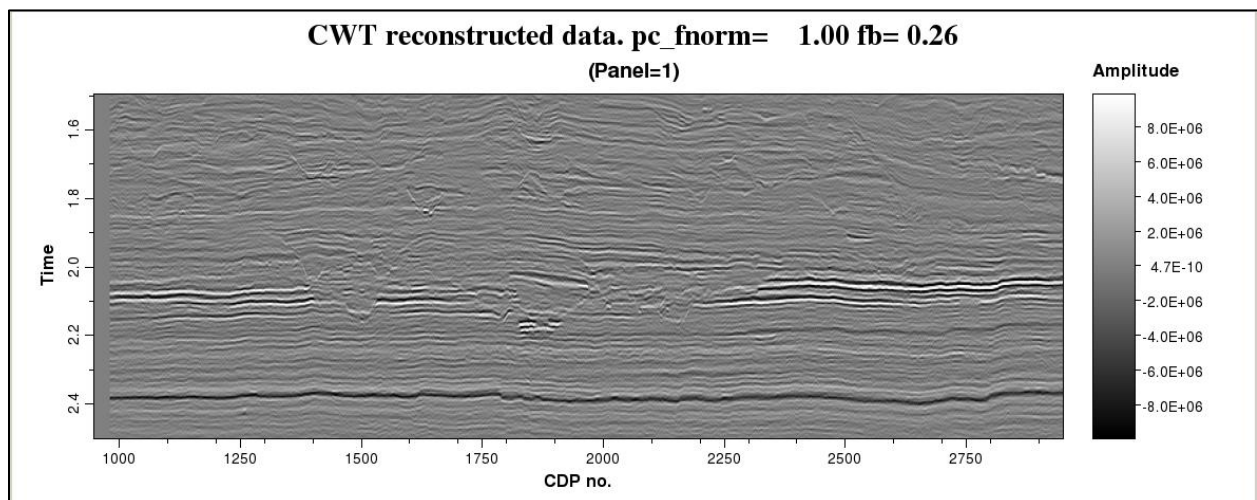


Figure 14.

Spectral Attributes: Program `spec_cwt`

The output of the next two options will be different.

Generating output about and between two horizons

In the example below, I chose the upper and lower horizons to be the same, thereby computing data about a single horizon but *without* flattening. The output data window is defined to be that of minimum and maximum of the two padded horizons:

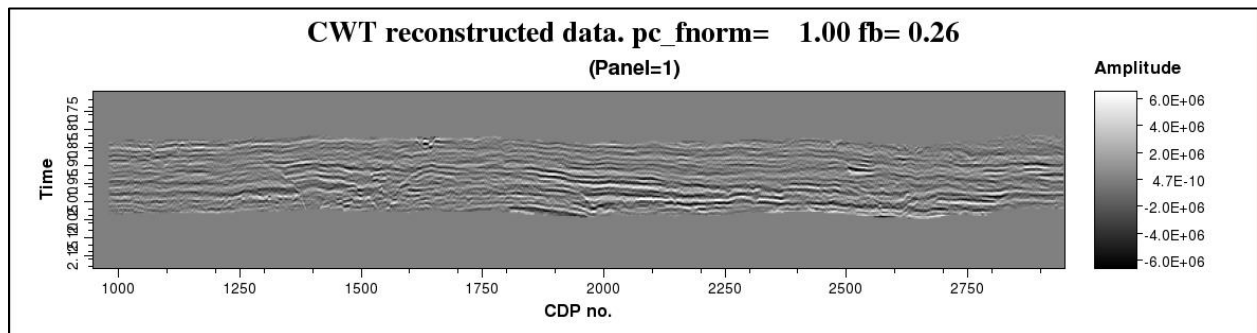
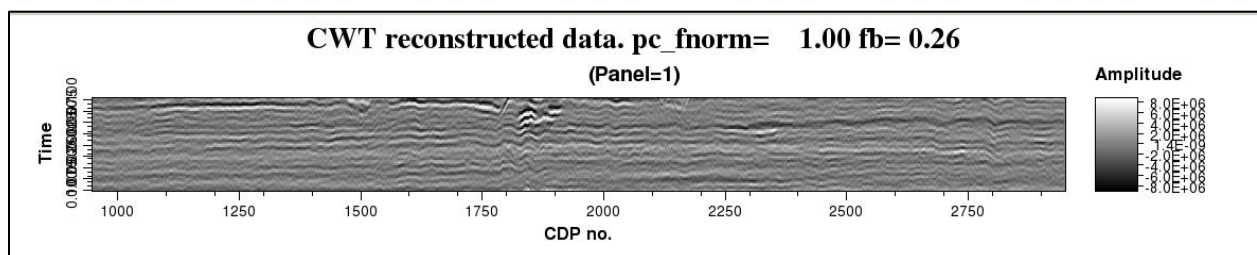


Figure 15.

Generating flattened output

The appearance and use of flattened spectral components and spectrally balanced seismic data is easy to understand but quite complicated to compute. Specifically, the AASPI developers believe that the use of spectral component tuning effects as an estimate of relative bed thickness should only be done on spectrally balanced data. If the data are not spectrally balanced, any reflector tuning effect will be overprinted by the non-flat shape of the effective seismic source wavelet. Because a picked horizon may have significant structural relief, this time-variant spectral balancing should be applied to the data before flattening. The algorithm therefore involves two steps. First, the spectra are computed on the unflattened data in temporal range that spans the padded horizon. Second, the entire input data volume is flattened, the spectra computed in the target area, and the scale corresponding to unflattened location is applied to the results. Flattening the entire data window implicitly provides sufficient data padding such that the results at the top and bottom of the output window are as accurate as at the center of the window.

The flattened, spectrally balanced, and reconstructed flattened seismic amplitude data along line 4000 of the Tui3D survey looks like this:



where the vertical axis ranges between -0.100 s and +0.100 s. Three representative spectral components along this same line look like this:

Spectral Attributes: Program `spec_cwt`

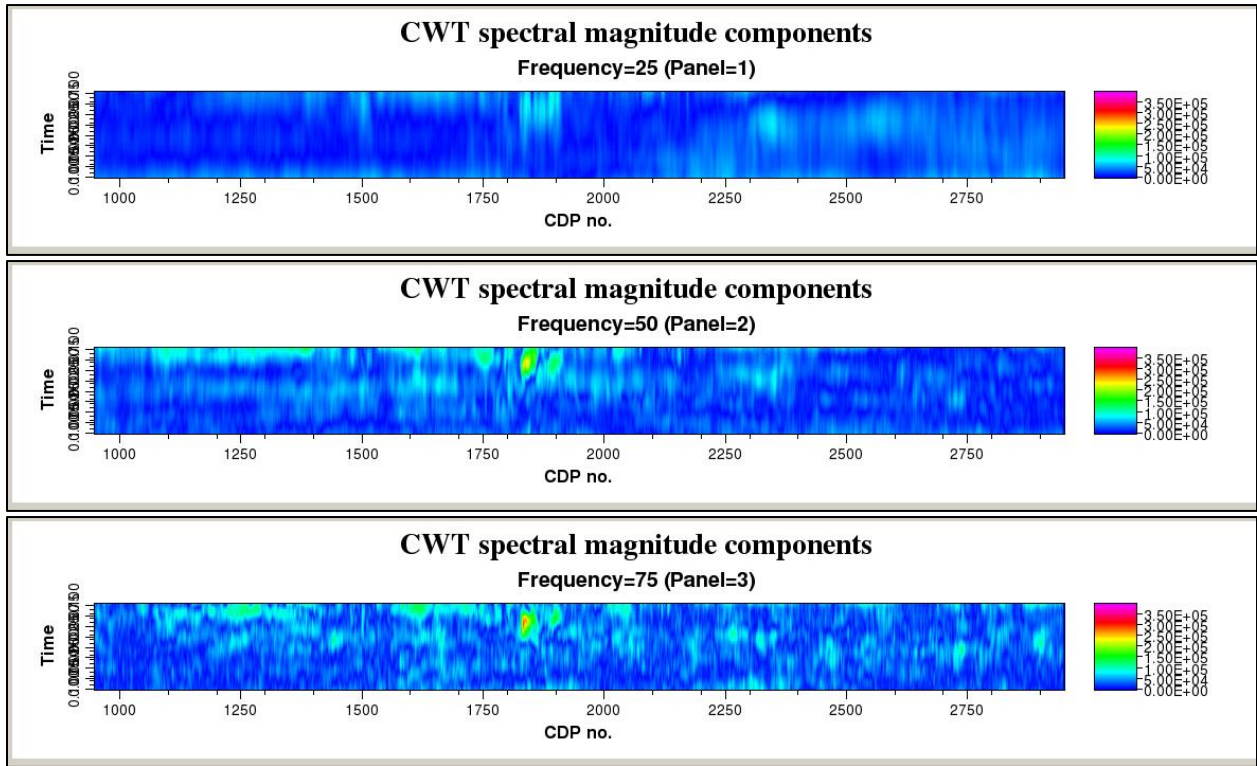


Figure 15. Vertical slices through three flattened subvolumes.

A representative time slice -0.080 s (above) the picked horizon through the three flattened spectral components of the Tui3D survey looks like this:

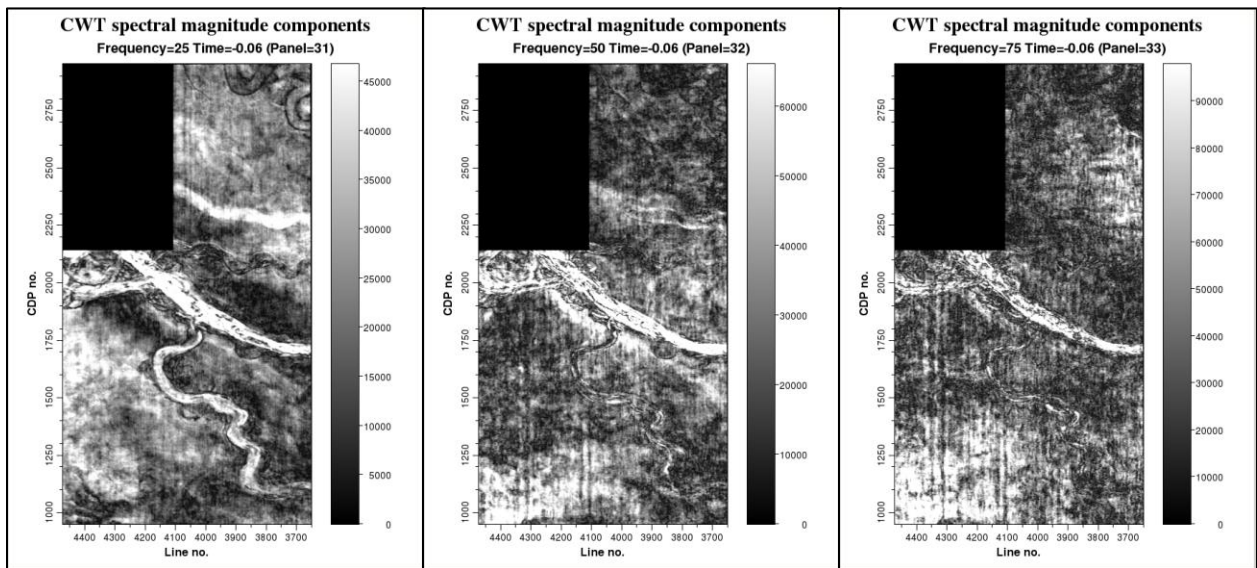


Figure 16. Time slices through three flattened spectral subvolumes.

Bandwidth extension

The AASPI implementation of bandwidth extension is based on Mallat and Zhong's (1992) concept of approximating the seismic response by convolving a wavelet with the maximum magnitude locations of the ridges in the CWT magnitude spectrum.

Theory: Bandwidth extension based on Wavelet Transform Maximum Magnitude Lines (WTMML)

Unlike spectral balancing whose objective is to equalize the contribution of each measured spectral component thereby improving resolution, bandwidth extension generates spectral components that fall above and below those of the measured data. The creation of these extended components is model-based, with the most common model being that of piecewise smoothly varying impedances whose interfaces are represented by a suite of discrete reflection events. Such "sparse spike" assumptions have long been used in seismic processing and form the underlying model of maximum entropy and other advanced deconvolution algorithms. Portniaguine and Castagna (2005) and Smith et al. (2008) show the interpretive value of bandwidth extension; however, their implementation details are proprietary. Here we implement a similar algorithm described by Matos and Marfurt (2011) based on work by Mallat and Zhong (1992) who showed that the original signal can be approximately reconstructed using a multiscale edge representation. Specifically, the bulk of the seismic response can be represented by the phase, $\varphi(t,f)$ and magnitude (or modulus) $a(t,f)$ of the complex spectral ridges at each spectral component,

$$D(t_k, f_j) = a(t_k, f_j) \exp[\varphi(t_k, f_j)], \quad (59)$$

where

$$t_k(f_j) = \text{ARG} \left\{ \text{MAX}_k [a(t_k, f_j)] \right\}, \text{ or} \quad (60)$$

$$d(t) \approx \sum_{j=1}^J \sum_{k=1}^{K(j)} D(u_k, f_j) \psi(t - u_k, f_j, f_B), \quad (61)$$

where the bandwidth, f_B , is the same as used in the forward transform. Mallat and Zhong (1992) called the maxima $a(t_k, f_j)$ or "ridges" the wavelet transform maximum modulus lines (WTMML). Improvements to the approximation given by equation 61 are achieved by iterating on the residual and by interpolating the input seismic data, thereby decreasing the temporal sample interval between samples, k . Bandwidth extension is then obtained by replacing the wavelets $\psi(t, f_j, f_B)$ with wavelets $\psi(t, f_j, f_B^{\text{broad}})$ having broader bandwidth. In our implementation, we use a percentage of the maximum magnitude of each trace to provide a threshold,

$$a_{\min} \equiv \varepsilon \text{MAX}_{k,j} [a(t_k, f_j)]. \quad (62)$$

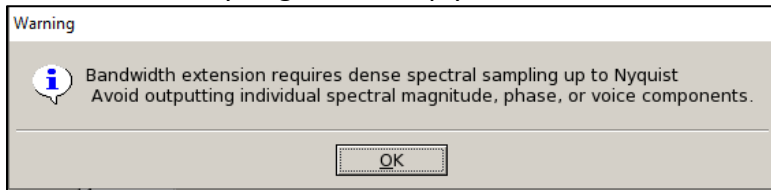
WTMML values greater than a_{\min} will be used in the reconstruction, while those less than a_{\min} will be discarded. The WTMML data using the forward CWT will be subtracted from the original data, forming a WTMML residual.

The major weakness of bandwidth extension is the underlying sparse spike model. Smith et al. (2008) teach that one should validate such a model by generating synthetic well ties with the original and bandwidth extended data. Improved correlation of the synthetic from the bandwidth extended data indicate the underlying model is valid and the bandwidth extended data can be used; conversely, decreased correlation indicates the underlying model is invalid and the bandwidth extended data should be rejected.

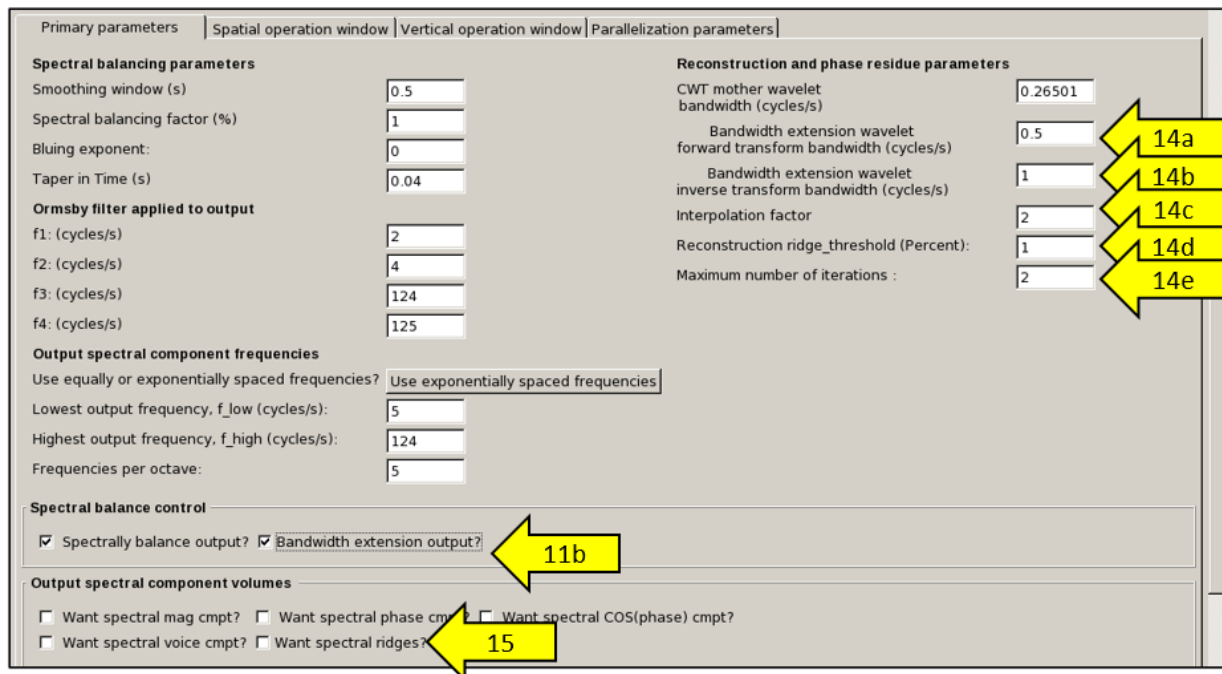
Spectral Attributes: Program `spec_cwt`

Bandwidth extension GUI parameters

To implement bandwidth extension (11b) place a checkmark in front of the *Bandwidth extension output?* option. A pop-up menu appears warning that the interpolated component results may be unreasonably large and fill up your disk.



If desired, modify the default spectral bandwidths for the (14a) forward and (14b) inverse CWT bandwidth extension transforms. In general, you will want to first (14c) interpolate the input seismic data to a finer sampling interval. Such interpolation results in more accurate computation of the wavelet transform maximum modulus lines (WTMMLs) as well as a necessary sampling rate to support the extrapolated higher frequency components. Be forewarned that the cost of computation increases with the amount of interpolation. Values of 2 or 4 are usually sufficient. Internal to the software, the actual values of the WTMMLs are interpolated to fractional sample values. The reconstruction (14d) ridge threshold a_{\min} is controlled by the value of ϵ in equation 62 expressed as a percentage. Finally, enter the (14e) number of desired iterations. If your test volume is small, you may wish to examine the (15) WTMML *spectral ridges* as well as some of the spectral magnitude and phase components.



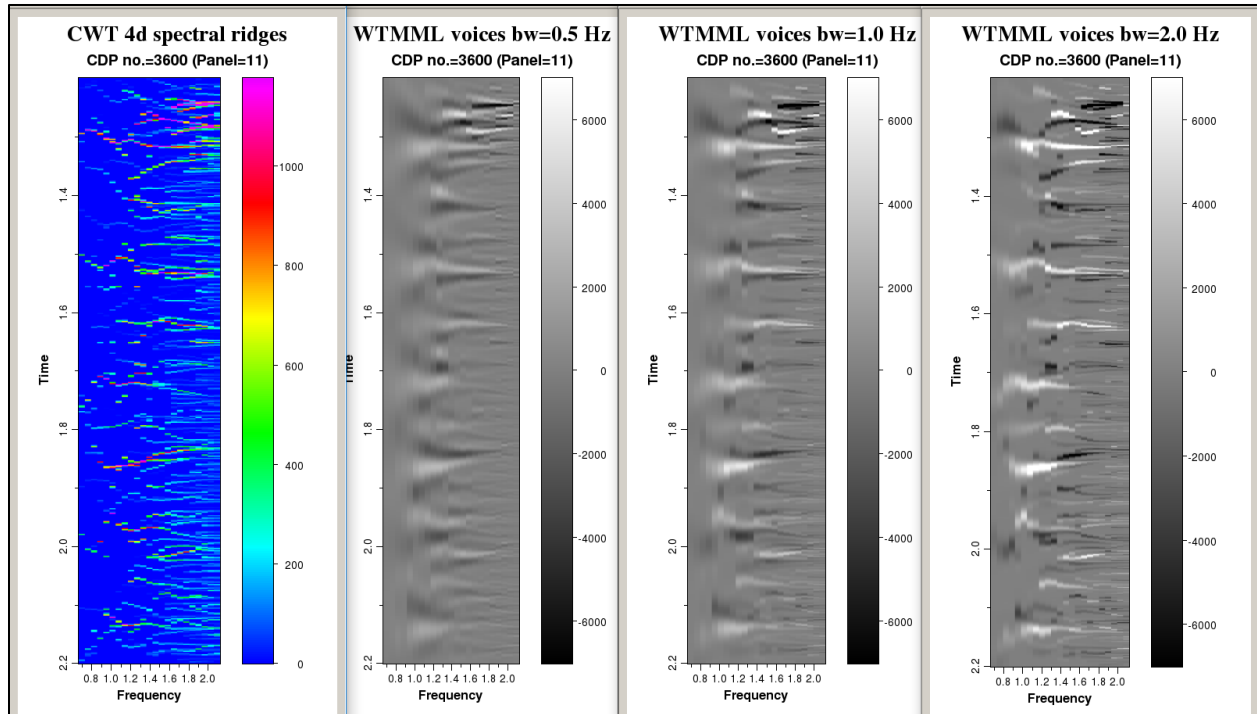


Figure 16. (a) Magnitude of the wavelet transform maximum magnitude lines (or ridges) for a representative trace. There is also a phase for each ridge. (b) The same WTMML ridges convolved with a family of wavelets with a mother wavelet bandwidth of $f_B=0.5$ Hz is used in the forward transform. Ridge magnitude and phases used in (a) and (b) but now reconstructed and there by extended using a mother wavelet bandwidth of (c) $f_B=1.0$ Hz, and (d) of $f_B=2.0$ Hz.

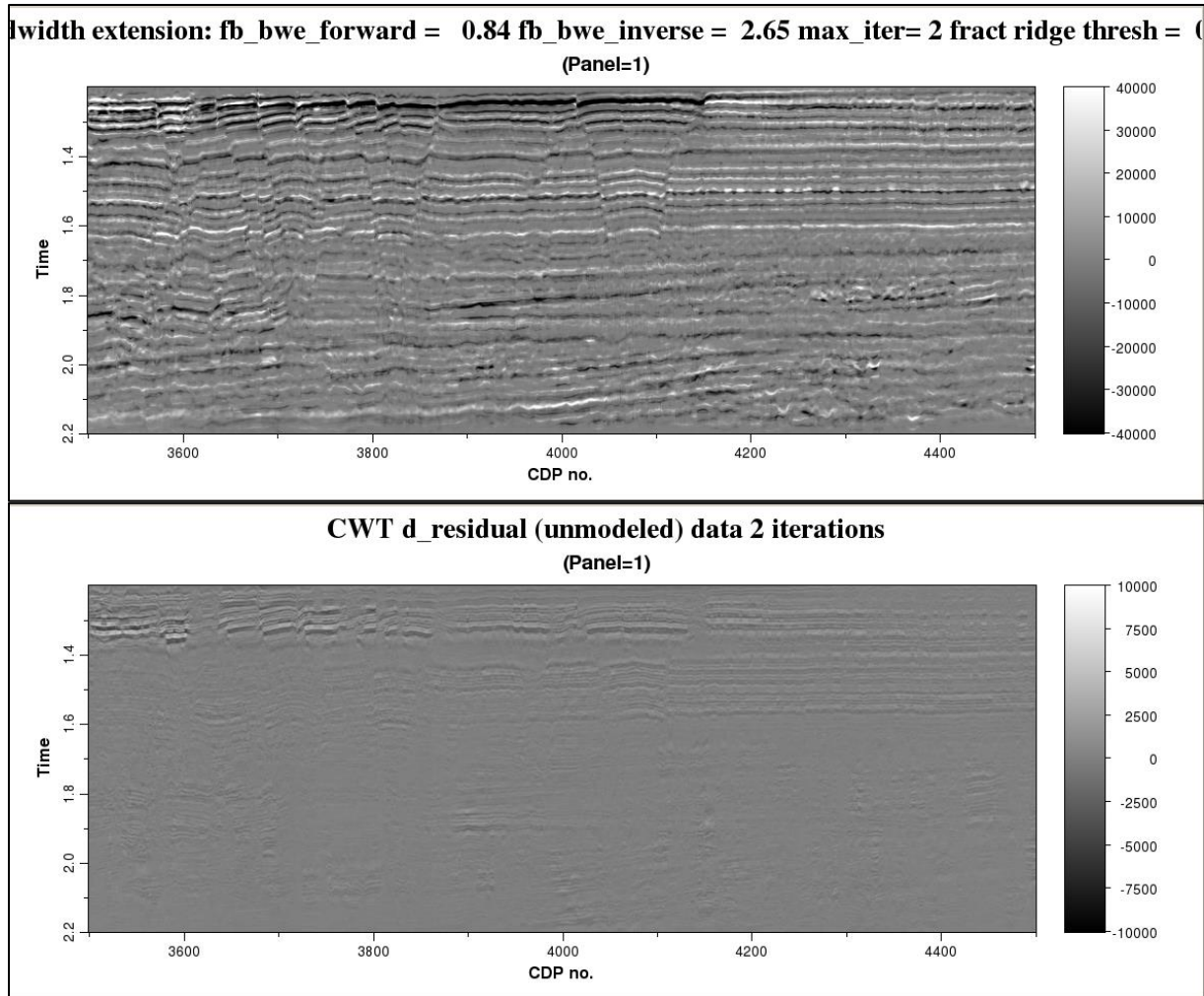


Figure 17. (a) Bandwidth extension and (b) the residual (unmodeled) data computed from the original (non-spectrally balanced data) after two iterations using a ridge threshold of 1.0%

Spectral Attributes: Program `spec_cwt`

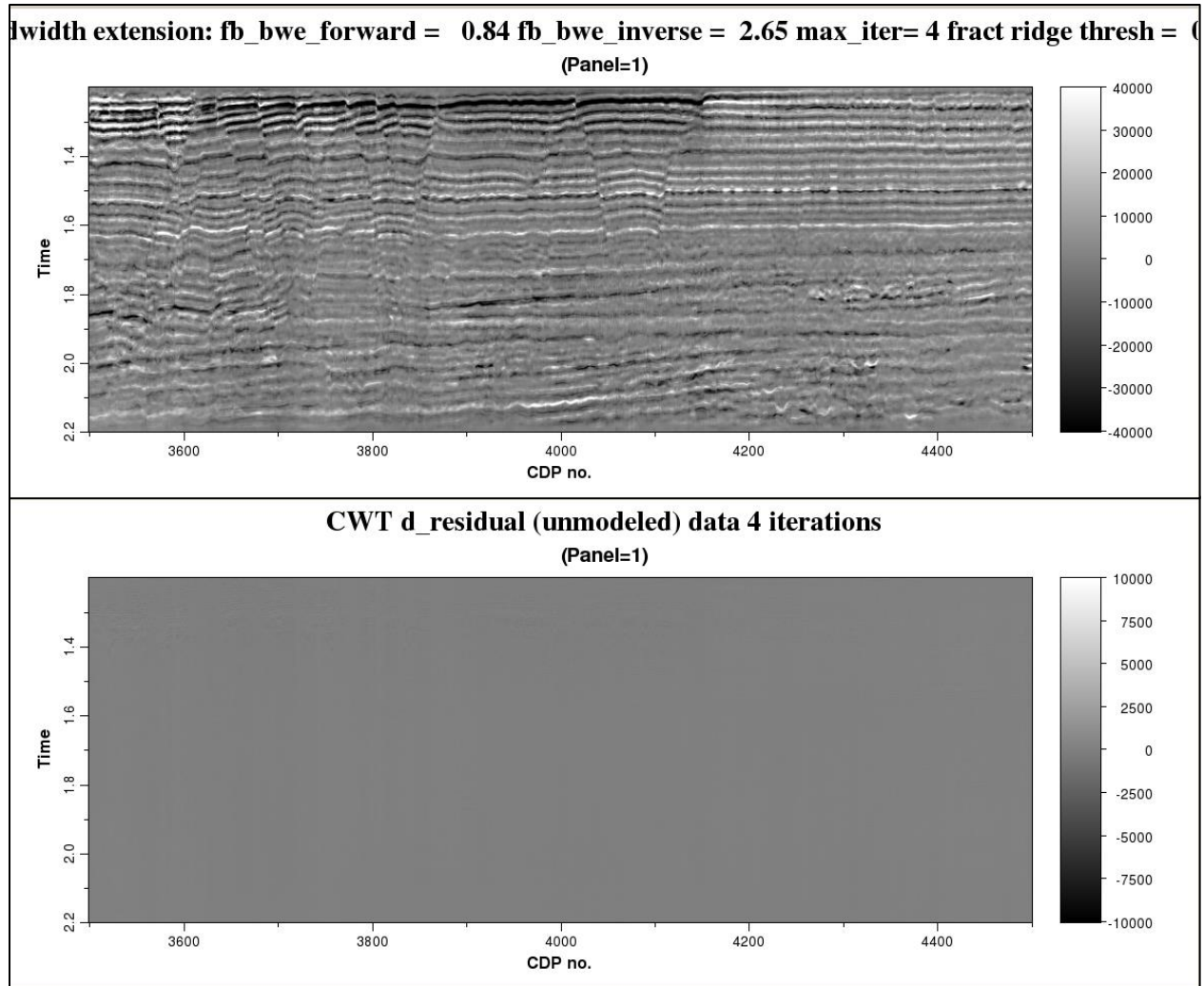


Figure 18. (a) Bandwidth extension and (b) the residual (unmodeled) data computed from the original (non- spectrally balanced data) after four iterations using a ridge threshold of 1.0%

Phase residues

In the last GUI image note (4) the *Want phase residue attributes?* option. The phase residue is a measure of discontinuities in the phase component of the seismic data. Examination of Figures 4 and 9 will reveal discontinuities in the phase. These discontinuities are referred to as “phase residues” (see gray box below) that are often associated with abrupt changes in geologic deposition. Similar spectral discontinuities in the spectral magnitude components form the basis of the “Spice” algorithm developed by Liner et al. (2006).

Theory: The Phase Residue

Ghiglia and Pritt (1998) provide an excellent survey of 2D phase-unwrapping techniques and show how a complex residue theorem based on vector calculus can be applied to the phase-unwrapping problem. They use a rectangular integration path aligned with the t and f axes. We choose a smaller diamond-shaped integration path about each sample (t_j, f_k) given by:

$$I_{jk} = \frac{W[\psi(t_{j-1}, f_k) - \psi(t_j, f_{k-1})]}{2\pi} + \frac{W[\psi(t_j, f_{k-1}) - \psi(t_{j+1}, f_k)]}{2\pi} + \frac{W[\psi(t_{j+1}, f_k) - \psi(t_j, f_{k+1})]}{2\pi} + \frac{W[\psi(t_j, f_{k+1}) - \psi(t_{j-1}, f_k)]}{2\pi} \quad (63)$$

where ψ is the phase and W is a wrapping operator that produces an output that falls between $\pm\pi$. If the integral I_{jk} in equation 24 is nonzero, there are inconsistent phase points, which Ghiglia and Pritt (1998) call “phase residues”. Figure A4 shows how the residue is calculated for a small portion of a typical wrapped time-frequency phase matrix.

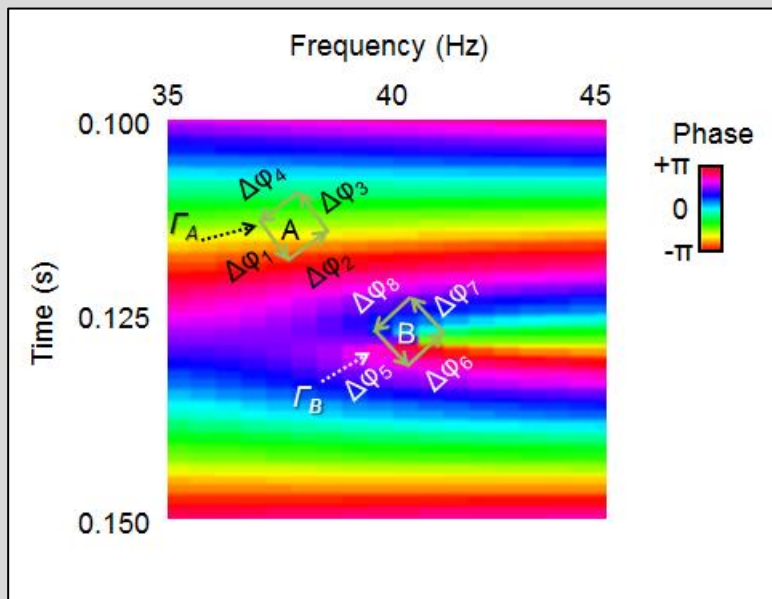


Figure A4. Diamond-shape integration paths used in computing the phase residue. Area A is continuous, with a phase residue = 0.0, while area B is discontinuous with a phase residue = 1.0 .

Matos et al. (2011) find spectral phase components to be sensitive to the same kinds of stratigraphic discontinuities seen by analyzing the spectral magnitude components; however, because phase is often a more accurate seismic measure than magnitude, it holds significant promise in mapping stratigraphic unconformities. Accurate computation of phase residues requires relatively fine sampling across frequency. We suggest sampling the spectrum with 5 frequencies per octave.

Spectral Attributes: Program `spec_cwt`

Figure 19 below shows the phase residues corresponding line 2701 of the *GSB_small* survey where the color represents the frequency of the residue and the saturation its magnitude.

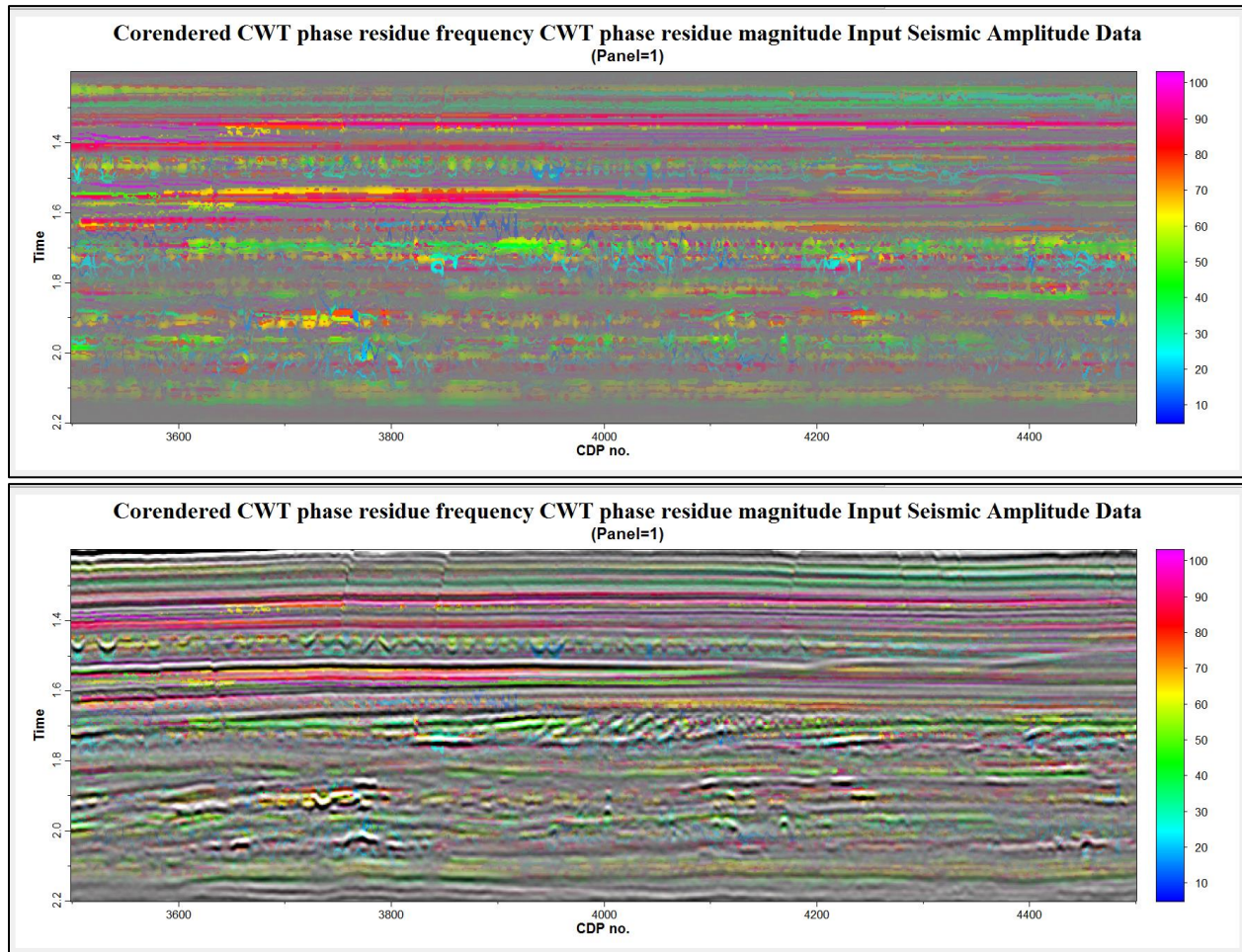


Figure 19. (a) The phase residues corresponding to the same vertical slice shown in Figure 9. (b) The same phase residues co-rendered with the original seismic amplitude data.

Example 3: Mapping incised channels using phase residues

This example comes from Davogustto et al.'s (2012) analysis of an incised Red Fork valley in the Anadarko Basin of Oklahoma. There were 660 wells within the seismic survey that provided detailed analysis that fell below seismic resolution.

Spectral Attributes: Program `spec_cwt`

Inola Limestone and pink picks are the Pink Limestone. Squares represent the well tops for each formation on each well. (After Davogustto et al., 2012).

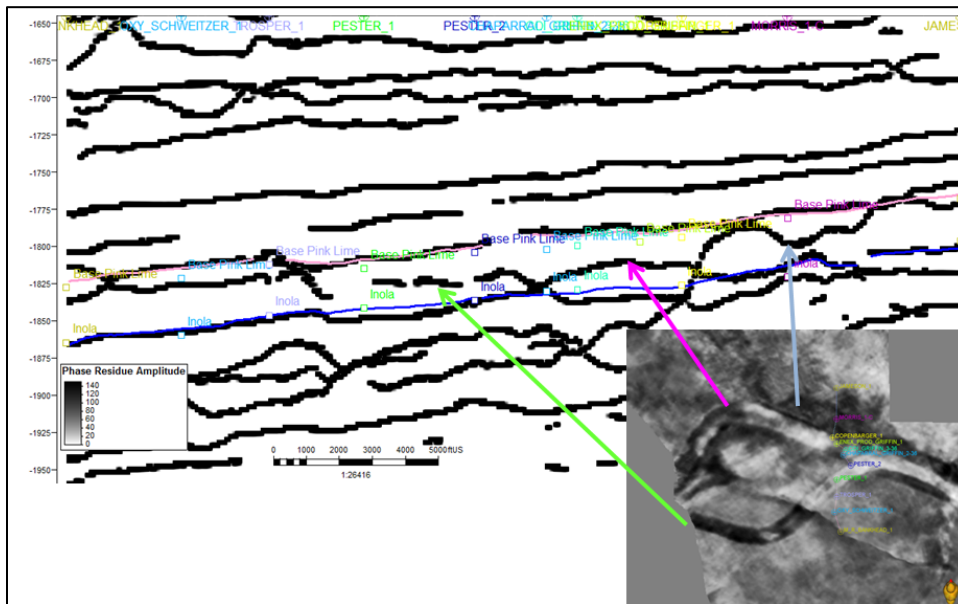


Figure 22. Phase residue magnitude on the same vertical section. Now we see anomalies that look like channels or in this case incision stages. The cyan arrow indicate stage 1 and 2, the purple arrow stages 3 and 4 and the green arrow stage 5. Well tops indicate the Pink and the Inola limestones. (After Davogustto et al., 2012).

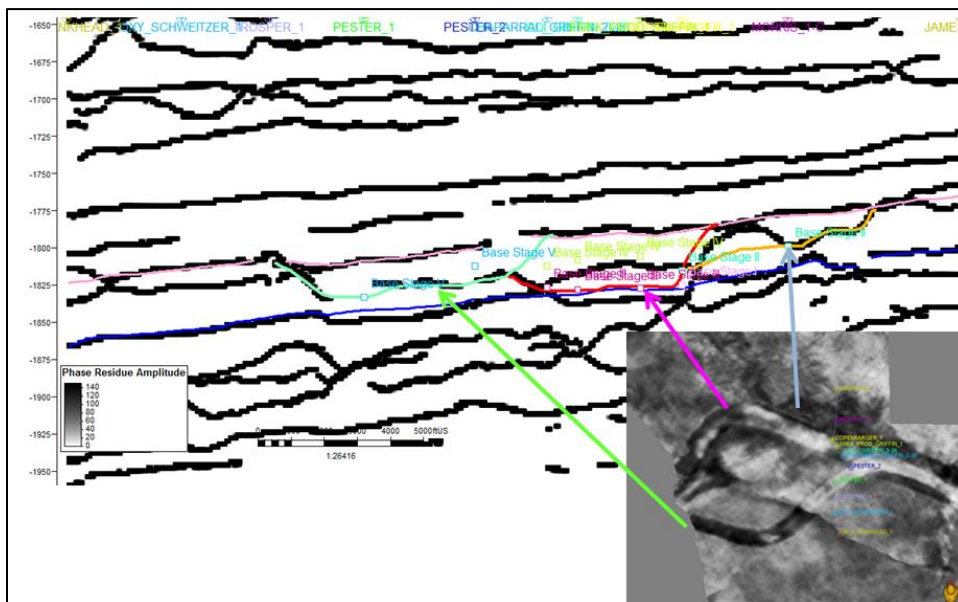


Figure 23. Using the tops from the logs Davogustto et al. (2012) proceed to interpret each of the anomalies. They are able to extract surfaces for each one of the stages from the attribute and use these to build the geological model.

Spectral Attributes: Program `spec_cwt`

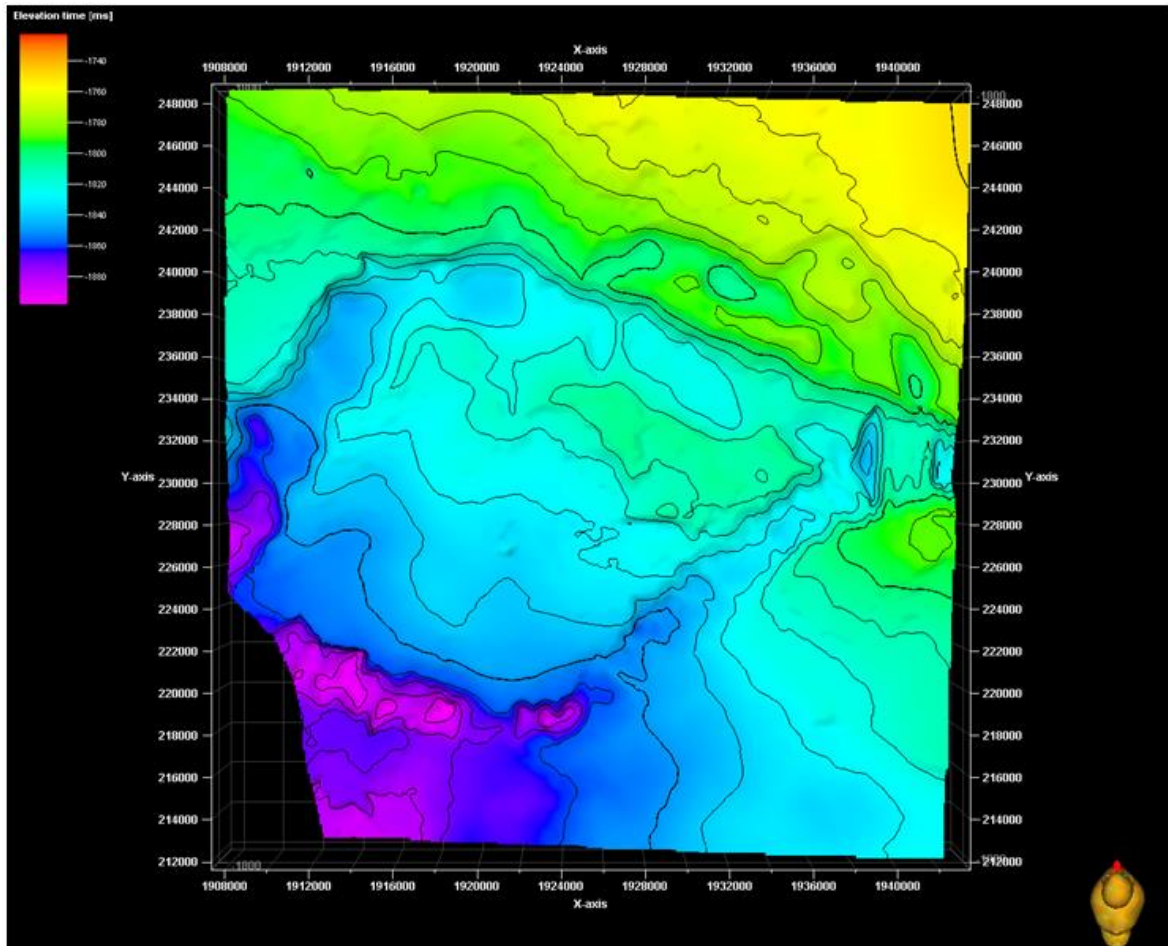


Figure 24. Time-structure map of the top Red fork computed by picking the conventional seismic amplitude volume. (After Davogustto et al., 2012).

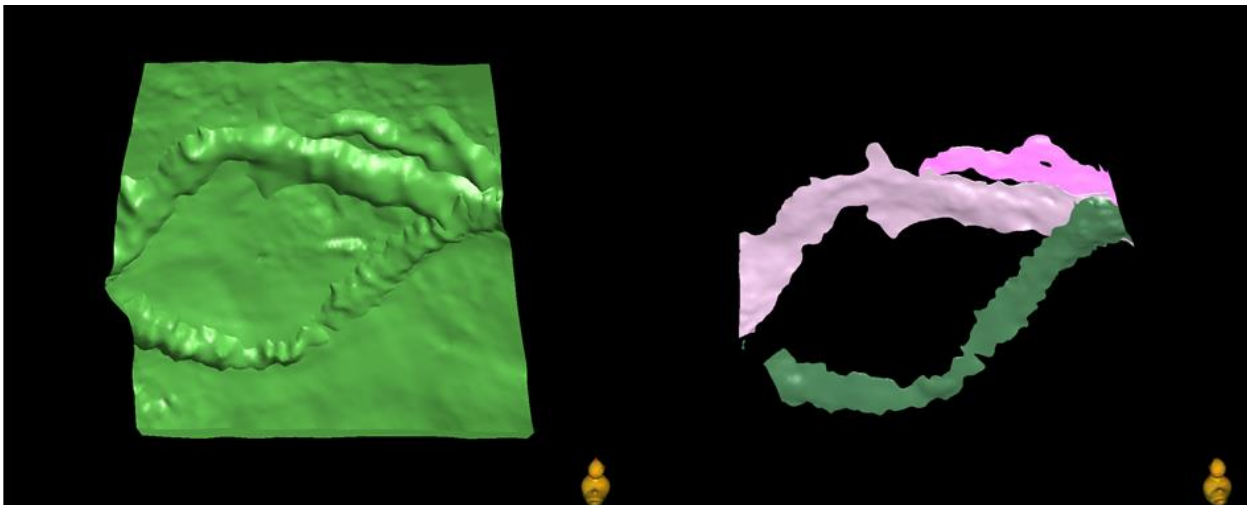


Figure 25. The resulting geomodel from the seismic interpretation. On the right is the regional Red Fork which corresponds to delta plains and marshes. Note each one of the stages of incision of the valley, simplifying subsequent construction of a geocellular model with geobody specific different net to gross or porosity schemes. (After Davogustto et al., 2012).

Spectral Attributes: Program `spec_cwt`

Computing coherence from different spectral components

The amplitude and phase of spectral components is a function of thickness and changes in reflection coefficients. Li et al. (2017) first computed a suite of spectral voice components at different frequencies. They then computed coherence from each of these voice components, finding that channels that were better tuned at a given frequency component produced improved channel edges using coherence. Three of these coherence images can be combined using program `aaspi_corender`. Such computations are of significant value that multiple coherence volumes as well as a multispectral coherence volume are now options in program `similarity3d`.

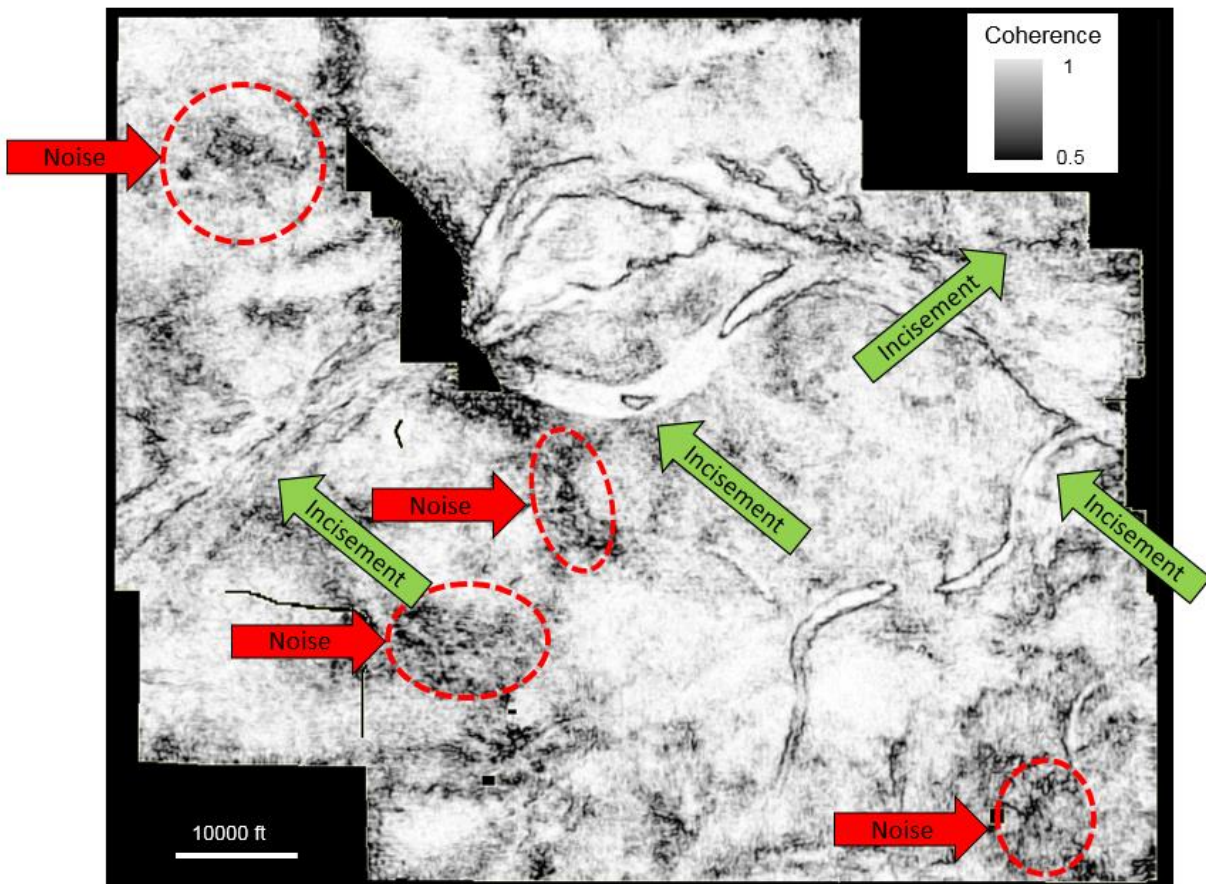


Figure 26.

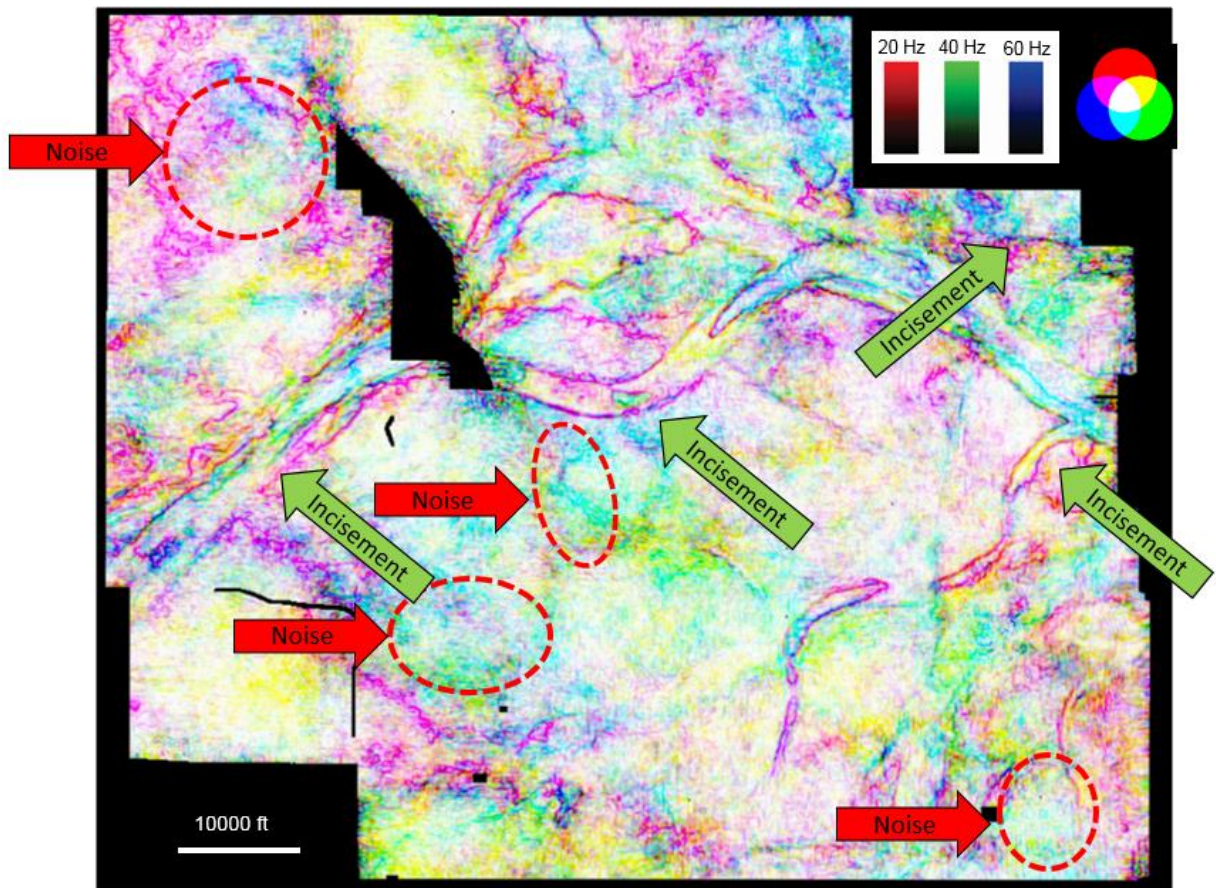


Figure 27. (Top) Broadband coherence, and (Bottom) corendered coherence volumes computed from 20 (red), 40 (green), and 60 (blue) Hz spectral voice components showing incised Redd Fork channels in the Anadarko Basin, OK. (After Li et al., 2017).

Spectral Attributes: Program `spec_cwt`

References

- Davogustto, O., M. Castro de Matos, and K. J. Marfurt, 2012, Using phase residues to map Red Fork channels: Geophysical Society of Oklahoma City Spring Expo.
- Davogustto, O., M. Castro de Matos, C. Cabarcas, T. Doan, and K. J. Marfurt, 2013, Resolving subtle stratigraphic features using spectral ridges and phase residues: Interpretation, **1**, SA93-SA108.
- Ghiglia, D., and M. D. Pritt, 1998, Two-dimensional phase unwrapping: Theory, algorithms, and software: Wiley-Interscience.
- Goupillaud, P., A. Grossman, and J. Morlet, 1984, Cycle-octave and related transforms in seismic signal analysis: Geoexploration, **23**, 85-102.
- Grossmann, A., and J. Morlet, 1984, Decomposition of Hardy functions into square integrable wavelets of constant shape: SIAM Journal on Mathematical Analysis, **15**, 723-736, doi:10.1137/0515056.
- Li, X. G., and T. J. Ulrych, 1999, Well log analysis using localized transforms, J. Applied Seismology, **8**, No. 3, 243-260.
- Li, C., and C. Liner, 2008, Wavelet-based detection of singularities in acoustic impedances from surface seismic reflection data: Geophysics, **73**, V1-V9
- Li, F. Y., and W. K. Lu, 2014, Coherence attributes at different spectral components: Interpretation, **2**.
- Liner, C., C.-F. Li, A. Gersztenkorn, and J. Smythe, 2004, SPICE: A new general seismic attribute: 72nd Annual International Meeting of the Society of Exploration Geophysicists, Expanded Abstracts, 433-436.
- Mallat, S., and S. Zhong, 1992, Characterization of signals from multiscale edges: IEEE Transactions on Pattern Analysis and Machine Intelligence, **14**, 710-732.
- Mallat, S., 2009, A wavelet tour of signal processing, 3rd ed.: Academic Press.
- Matos, M. C., and K. J. Marfurt, 2011, Inverse continuous wavelet transform “deconvolution”: 81st Annual International Meeting, SEG, Expanded Abstracts, 1861-1865.
- Marfurt, K., 2018, Seismic Attributes as the Framework for Data Integration throughout the Life of the Oilfield, The Society of Exploration Geophysics.
- Matos, M. C., O. Davogustto, K. Zhang, and K. J. Marfurt, 2011, Detecting stratigraphic discontinuities using time-frequency seismic phase residues: Geophysics, **76**, P1-P10.
- Morlet, J., G. Arens, E. Fourgeau and D. Giard, 1982, Wave propagation and sampling theory - Part II: Sampling theory and complex waves, Geophysics, **47**, 222-236.
- Neep, J. P., 2007, Time variant colored inversion and spectral bluing: 69th EAGE Annual Meeting, Extended Abstracts, B009.
- Peyton, L., R. Bottjer, and G. Partyka, 1998, Interpretation of incised valleys using new 3D seismic techniques: A case history using spectral decomposition and coherency: The Leading Edge, **17**, 1294-1298.
- Portniaguine, O. and J. P. Castagna, 2005, Spectral inversion: lessons from modeling and Boonsville case study, SEG Expanded Abstracts, 1638-1641.
- Singleton, S.W., M.T. Taner, and S. Treitel, 2006, Q-estimation using Gabor-Morlet joint time-frequency analysis: 76th Annual International Meeting, SEG, Expanded Abstracts, 1610-1614.

Spectral Attributes: Program **spec_cwt**

Smith, M., G. Perry, J. Stein, A. Bertrand, and G. Yu, 2008, Extending seismic bandwidth using the continuous wavelet transform: *First Break*, **26**, 97-102.

Taner, M. T., F. Koehler, and R. E. Sheriff, 1979, Complex seismic trace analysis: *Geophysics*, **44**, 1041-1063.

Teolis, A., 1998, *Computational Signal Processing with Wavelets*, 1st ed: Birkhäuser Boston.

Zhang, K., K. J. Marfurt, and Y. Guo, 2008, Volumetric application of skewed spectra: 78th Annual International Meeting, SEG, Expanded Abstracts, 919-923.